Renormalization of chiral two-pion exchange NN interactions with Δ excitations: Correlations in the partial-wave expansion

M. Pavon Valderrama*
Institut für Kernphysik and Jülich Center for Hadron Physics, Forschungszentrum Jülich, D-52425 Jülich, Germany

E. Ruiz Arriola†
Departamento de Física Atómica, Molecular y Nuclear, Universidad de Granada, E-18071 Granada, Spain.
(Received 5 June 2010; revised manuscript received 17 February 2011; published 29 April 2011)

In this work we consider the renormalization of the chiral two-pion exchange potential with explicit Δ excitations for nucleon-nucleon scattering at next-to-leading (NLO) and next-to-next-to-leading order (N^2LO). Because of the singular nature of the chiral potentials, correlations between different partial waves are generated. In particular, we show that two-body scattering by a short distance power like singular attractive interaction can be renormalized in all partial waves with a single counterterm, provided the singularities are identical. A parallel statement holds in the presence of tensor interactions when the eigenpotentials in the coupled channel problem also coincide. Although this construction reduces the total number of counterterms to 11 in the case of nucleon-nucleon scattering with chiral two-pion exchange interactions with Δ degrees of freedom, the differences in the scattering phases as compared to the case with the uncorrelated partial-wave renormalization become smaller as the angular momentum is increased in the elastic scattering region.

DOI: 10.1103/PhysRevC.83.044002 PACS number(s): 13.75.Cs, 03.65.Nk, 11.10.Gh, 21.30.Fe

I. INTRODUCTION

The basic and fundamental problem of nuclear physics is the determination of the nucleon-nucleon (NN) interaction [1]. Field theoretical approaches to the nuclear force state that the NN potential can be expressed as a sum of increasingly heavy meson exchange contributions (for reviews see, e.g., [2,3] and references therein). The resulting high-quality potentials describe neutron-proton and proton-proton scattering data with a $\chi^2/\text{d.o.f.} \leqslant 1$ [4–7]. They all include at large distances the charge-dependent one-pion exchange (OPE) potential and typically need on the order of 40 parameters for parametrizing the shorter range components of the interaction. On the contrary, quantum chromodynamics (QCD), the underlying fundamental theory of the strong interaction, requires only two parameters in the isospin symmetric limit: Λ_{QCD} and the average up and down quark masses. These fundamental QCD parameters can be traded for experimentally accessible observables such as f_π, the pion weak decay constant, and m_π, the averaged pion mass. Obviously, the large number of parameters needed in phenomenological approaches arises within very specific schemes and functional forms. It is not clear whether this number of parameters can effectively be reduced by invoking relevant QCD features while maintaining the quality of the description at the same time. Ultimately, lattice *ab initio* calculations of the NN potential, for which incipient results already exist [8,9], will eventually solve the problem.

In the present paper we deal with a situation where a reduction of parameters arises within the context of the renormalization of the chiral potentials deduced from the effective field theory (EFT) approach suggested by Weinberg [10] two decades ago (for comprehensive reviews, see Refs. [11,12]). These chiral potentials turn out to be singular interactions which exhibit an inverse power law behavior $\sim 1/r^n$ at distances below the pion Compton wavelength, $m_\pi r \ll 1$. In case they are attractive the resulting amplitudes are sensitive to short distance physics and require renormalization. As will be shown, the renormalizability of singular attractive potentials can be translated into a mathematical short distance constraint on the scattering amplitude for different partial waves. In the simplifying case of two-body scattering by a central attractive singular potential only one counterterm is needed to renormalize all the partial waves. In the more complex case of NN scattering, where spin, isospin dependence, and tensor forces are present, this number can rise to 11 counterterms provided that certain conditions are met. We review below the EFT approach from the perspective of the number of parameters in a way that our results can easily be displayed.

The main appeal of the EFT idea in nuclear physics lies in the promise of a model independent approach where the long- and short-range contributions to observables can be disentangled with the aid of a sensible hierarchy, eluding the ubiquitous problem of fine tunings. This feature is explicitly displayed through the introduction of counterterms in the effective Lagrangian, which encode the underlying but unresolved short distance physics and are organized according to a power counting. The standard EFT formulation of the nuclear forces exploits the spontaneous breakdown of chiral

*m.pavon.valderrama@fz-juelich.de; Present address: Departamento de Física Teórica and Instituto de Física Corpuscular (IFIC), Institutos de Investigación de Paterna, Aptd. 22085, E-46071 Valencia, Spain.
†earriola@ugr.es

symmetry, which requires derivative couplings for the pion. This implies that higher pion exchanges are power suppressed at momenta which are small compared with the chiral scale $\Lambda_\chi \sim (4\pi f_\pi, M_N) \sim 1$ GeV. On the contrary, at high virtual momenta, pion exchanges become large, eventually requiring a suitable renormalization through the introduction of counterterms. Furthermore, the nonperturbative nature of the *NN* interaction makes using a sensible resummation of diagrams mandatory. A simple and effective method already suggested by Weinberg [10,13] and implemented for the first time by Ray, Ordóñez, and van Kolck [14,15] proceeds in two steps: First, one deduces a chiral nuclear potential and afterward solves the corresponding Lippmann-Schwinger equation in momentum space, or equivalently, the Schrödinger equation in coordinate space. This scheme complies to the familiar and widely accepted concept of nuclear potential, which in the chiral case can be organized as an expansion in powers of Q [16–26]:

$$V(r) = V_\chi^{(0)}(r) + V_\chi^{(2)}(r) + V_\chi^{(3)}(r) + V_\chi^{(4)}(r) + \mathcal{O}(Q^5), \tag{1}$$

where Q represents either the pion mass or the momentum of the nucleons (or additionally the nucleon-Δ splitting in case we include the Δ excitation as an explicit degree of freedom). Within this scheme and making use of finite cutoffs at N^{3}LO [27,28], the number of parameters becomes comparable with that of the phenomenological potentials even though the long distance behavior is determined by chiral symmetry.

A stringent constraint follows from the natural requirement of short distance insensitivity: Physics not explicitly taken into account should be under control by fixing a sufficient amount of low-energy parameters. Such a condition represents the basis of the renormalization process as understood in the present work.[1] To fulfill this goal it is necessary to achieve approximate cutoff independence over a certain cutoff region. This immediately raises the question of what cutoff values can be regarded as natural and how much the *a priori* arbitrary cutoff can be varied. The shortest de Broglie wavelength probed in elastic *NN* scattering below pion production threshold is $\lambda_{\min} \sim 0.5$ fm, and thus we might expect stable results for similar short distance cutoffs. Otherwise the cutoff becomes an essential parameter of the theory. This particularly applies when the cutoff must be fine tuned to physical observables, a situation which actually takes place for specific power counting schemes.

By naive power counting one expects chiral potentials to be singular for $r \ll 1/m_\pi$[2],

$$V(r) \to \frac{1}{\Lambda_\chi^{\nu+2} r^{\nu+3}}, \tag{2}$$

where ν represents the order in the chiral expansion[3] [see Eq. (1)]. While the resummations implied by solving the wave equation mix up the chiral power counting, they also enable finding nonperturbative new features when the short distance cutoff r_c becomes much smaller than any other long distance length scale. There arises the possibility of finding the adequate number of counterterms which is compatible with the power counting of the long-range potential and of obtaining a finite and unique limit for the corresponding scattering amplitude. In this regard several studies have found that the original Weinberg power counting is inconsistent with renormalizability [29,35,36]. This unexpected result has suggested several alternative approaches and heated debates questioning the particular power counting, the renormalization process itself, or the correctness of the nonperturbative resummation. We will not ponder the pros and cons of any particular approach as this was already done from several viewpoints in Refs. [29,31,32,35,37]. At present it is unclear what aspects of the original EFT framework will ultimately prevail or be universally accepted by the nuclear physics community (in this regard, see the related discussion in Ref. [38]). Rather than considering the problem solved, we think that further work is still needed to settle the issue.

In previous works [35,36,39–41] we have shown that the necessary minimum number of counterterms renormalizing a singular interaction can in fact be determined *a priori* from the behavior of the configuration-space potential near the origin (for an earlier coordinate space treatment, see Ref. [42]). On a more numerical basis, similar observations have been made in momentum space either using finite cutoffs [29,41] or subtractive methods [43–46]. The main result is that in any uncoupled partial wave where an attractive singular potential is present, a counterterm is needed to renormalize this particular partial wave. An interesting corollary is that finite cutoff effects are less important the more singular the potential. Indeed, at order ν in the chiral counting the potential behaves as $1/\Lambda_\chi^{\nu+2} r^{3+\nu}$, generating finite cutoff corrections $\delta_\Lambda(k)$ to the renormalized phase shifts $\delta_\infty(k)$ which scale as

$$\delta_\infty(k) - \delta_\Lambda(k) = \mathcal{O}(\Lambda^{-5/2-\nu/2}), \tag{3}$$

for large enough cutoffs [40,41], meaning in particular that cutoff independence is achieved in this case. On the contrary, if

[1] By renormalization we specifically mean the existence of well-defined scattering amplitudes when the cutoff is removed. This condition allows one to identify all the short distance operators needed to remove the cutoff dependence, as done, for example, in Ref. [29] for the OPE case. Once these counterterms are included in the computation approximate cutoff independence is assured and consequently there is no problem in keeping a finite cutoff. For a different view on renormalization within an effective field theory context, see Lepage [30] and the related discussions of Refs. [31,32].

[2] The operator product expansion for six quark operators predict the functional form of the *NN* potential at short distance, which turns out to be a little weaker than $1/r^2$ and repulsive [33,34]. This shows that the *NN* potential computed on the lattice is regular and hence might predict uniquely the *NN* scattering data as well as the deuteron properties and also that this short distance dependence is quite different from the chiral potentials.

[3] The inclusion of static degrees of freedom, such as the Δ isobar excitation in the small scale expansion, can change the expected power law behavior of the potential.

the potential is singular and repulsive the effect of counterterms becomes negligible for small enough cutoff radii.

A particularly problematic consequence of the nonperturbative treatment of singular potentials is that the renormalization of two-body scattering by an attractive singular central interaction requires an infinite number of counterterms, one per each partial wave. The unlimited proliferation of counterterms when renormalizing singular interactions was, among others, an argument against removing the cutoff, as the resulting effective field theory will be unable to predict observables [31]. This problem can be cured in perturbative power countings, like the one proposed by Kaplan, Savage, and Wise [47,48], where the proliferation of counterterms is naturally limited by the order of the approximation. Unfortunately the singularity in the tensor forces makes the previous proposal poorly convergent in the ${}^3S_1 - {}^3D_1$ channel [49] (see, however, [50] for a renewed formulation). In the modified Weinberg proposal of Nogga, Timmermans, and van Kolck [29], OPE is iterated in low angular momentum waves while treated perturbatively in sufficiently peripheral waves (usually $l > 2$). This choice naturally limits the number of necessary counterterms and, although it was criticized as arbitrary in Ref. [31], it is sustained by the perturbative analysis of Ref. [37]. Higher order corrections are treated in perturbation theory and the corresponding (finite) number of counterterms is determined by imposing cutoff independence on the results, generating convergent amplitudes for the central waves with the NLO and N^{2}LO chiral potentials [51]. However, as we will show, there is a nonperturbative way of also obtaining a finite number of counterterms.

In a recent paper [52] we have analyzed the role of Δ degrees of freedom for the central waves and the deuteron with the chiral Δ potentials of Refs. [17,53] with a reasonable phenomenological success. This particular potential furnishes *simultaneously* the theoretical requirements of renormalizability[4] and power counting. Actually, convergence is achieved for reasonable cutoffs of the order of $r_c \sim 0.5$ fm, that is, scales comparable with the shortest wavelength probed in *NN* elastic scattering below pion production threshold.[5] Moreover, as discussed in Ref. [56], it may provide a good starting point for nuclear matter calculations as it has a rather small *D*-state probability, implying a sufficiently small wound integral which insures better convergence properties for the few body correlations and the nuclear many-body problem.

In the present work we analyze further the TPE potential with Δ excitations [17,53], addressing the calculation of noncentral partial waves. We show how the number of counterterms can be made finite by implementing a renormalization prescription correlating an infinite number of partial waves. Thus, this is a compelling example where, contrary to naive expectations, singular potentials may be consistently renormalized with a single common counterterm for *all* partial waves. The idea behind such a procedure is quite simple: If the potential has an inverse power law behavior at short distances, $V(r) \sim C/r^n$, with a coefficient C independent of energy and angular momentum, we expect all the reduced wave functions of the system to behave the same way at small enough radii, regardless of the energy or the angular momentum, as the contribution from these two factors will become negligible in comparison with the strength of the potential. As a trivial consequence, all partial waves can be related to the zero energy *s* wave. The issue is analyzed in detail in Sec. II both for regular and singular potentials. Although this becomes a relevant observation for uncoupled channels, the tensor force requires a suitable generalization of the result for coupled channels, which is discussed in Sec. III. Surprisingly, the potentials computed in Refs. [17,53] including TPE with Δ excitation do fulfill the necessary mathematical conditions to link partial waves with different angular momenta (see Sec. IV). Actually, we can estimate the finite cutoff error induced by these angular momentum correlations and which are exclusive of singular potentials. Other potentials do not automatically comply with these requirements, so the question on the consistency of the partial-waves correlations is not independent of the potential and indirectly on the power counting invoked to compute it. Of course, mathematical consistency does not necessarily mean phenomenological success, and we test our proposal against the widely accepted partial-wave analysis (PWA) of the Nijmegen group in Sec. V. We see that actually there is no big difference between using the finite number of counterterms or renormalizing independently wave by wave, suggesting that improvements might be sought in the TPE chiral potentials as well. For completeness we address the problem of the familiar OPE in Appendix A. Finally, in Sec. VI we summarize our main results and present our main conclusions and outlook for further work.

As in previous works [35,36,39–41] we use extensively the coordinate space formulation, which greatly simplifies the treatment and allows handy analytical calculations. In this approach, contact operators are treated implicitly via boundary conditions in coordinate space. We do not follow an *a priori* power counting for the contact operators, but rather deduce the short-range operator structure from the condition of cutoff independence and assuming that the long-range potential is to be fully iterated. The equivalence to momentum space renormalization was discussed in detail for scattering states in Ref. [41] and the deuteron in Ref. [55].

II. CENTRAL DELTA-SHELL POTENTIALS AND THE PARTIAL-WAVE EXPANSION

As a preparation we will consider first the simplest two-body scattering problem described by a central potential V,

[4]The divergence structure of this potential is identical to that of the chiral quark model in the Born-Oppenheimer approximation [54], which being second order perturbation theory provides only attractive and singular potentials.

[5]This is a purely coordinate space argument where the cutoff in the potential was removed. In momentum space the corresponding cutoff $\Lambda \sim \sqrt{m_\pi M_N} \sim 350$ MeV implies also a regularization of the potential and an effective quenching of the $g_{\pi NN}$ coupling constant. This might be one of the reasons why momentum space calculations renormalizing the LS equation [41,55] require much larger cutoffs $\Lambda \sim 1 - 4$ GeV than naively expected.

which for the l wave reads

$$-u''_{k,l}+\left[2\mu V(r)+\frac{l(l+1)}{r^2}\right]u_{k,l}(r)=k^2u_{k,l}(r), \quad (4)$$

where $u_{k,l}$ is the reduced wave function, μ the reduced mass of the system, and $k=\sqrt{2\mu E}$ is the center-of-mass momentum. The asymptotic long distance boundary condition is taken as

$$u_{k,l}(r)\to\sin\left[kr-\frac{l\pi}{2}+\delta_l(k)\right], \quad (5)$$

where $\delta_l(k)$ is the corresponding phase shift. We assume that $V(r)$ can be decomposed as the sum of a finite range potential V_F (bounded by an exponential fall-off $\sim e^{-mr}$) and a contact range interaction V_C,

$$V(r)=V_F(r;r_c)+V_C(r;r_c), \quad (6)$$

where we have added the auxiliary cutoff scale r_c, which will be needed to regularize the contact range interaction. For convenience we have also regularized the finite range potential in the following way:

$$V_F(r;r_c)=V_F(r)\theta(r-r_c), \quad (7)$$

which means that the short-range components of the finite range potential are effectively absorbed in the contact potential V_C. For the contact potential we only consider for definiteness the case in which V_C is a delta-shell interaction,

$$V_C(r;r_c)=\frac{C_0(r_c)}{4\pi r^2}\delta(r-r_c), \quad (8)$$

where C_0 does not depend on energy, and no higher derivatives of the delta function are considered. This is the simplest possible contact interaction and it actually becomes equivalent to a short distance boundary condition. We analyze below what can be obtained with such an interaction when the cutoff r_c is removed, both in the case of regular and singular interactions.

A. Delta-shell potentials and regular interactions

As mentioned, the two-body scattering problem can be described by the corresponding reduced Schrödinger equation [Eq. (4)]. For radii below the cutoff r_c, there is no potential [because of the specific regularization employed for the finite range piece of the potential; see Eq. (7)] and the solution for the wave function is simply

$$u_{k,l}(r)=const\times r^{l+1} \quad \text{for } r<r_c, \quad (9)$$

where the regular solution was chosen.

The solution for radii above the cutoff depends (i) on the size of the cutoff with respect to the range of V_F and (ii) on whether V_F is a regular or singular interaction. For the present discussion, we will assume that the cutoff is much smaller than the range of V_F, which we will call a_F, $r_c\ll a_F$, and that the finite range potential is a regular one, $\lim_{r\to 0}r^2V_F(r)=0$. Under these conditions the reduced wave function can be written as a linear combination of a regular and irregular solution for $r>r_c$, that is,

$$u_{k,l}(r)=a_l u^{(\mathrm{reg})}_{k,l}(r)+b_l u^{(\mathrm{irr})}_{k,l}(r) \quad \text{for } r>r_c, \quad (10)$$

where the superscripts $^{(\mathrm{reg})}$ and $^{(\mathrm{irr})}$ denote the regular and irregular solutions, respectively.

For small radii, say $r_c<r\ll a_F$, the behavior of the regular and irregular wave functions is given by

$$u^{(\mathrm{reg})}_{k,l}(r)\sim r^{l+1}, \quad (11)$$

$$u^{(\mathrm{irr})}_{k,l}(r)\sim\frac{1}{r^l}, \quad (12)$$

where corrections depending on the presence of the potential V_F or the finite momentum k do not appear until higher relative powers of r are considered.

The effect of the delta-shell potential in the Schrödinger equation, Eq. (4), is to generate a discontinuity in the first derivative of the reduced wave function at $r=r_c$. The previous statement can be summarized in the following relation between the logarithmic derivatives of the wave functions for $r<r_c$ and $r>r_c$,

$$\frac{2\mu C_0(r_c)}{4\pi r_c^2}=\frac{a_l(r_c)u^{(\mathrm{reg})'}_{k,l}(r_c)+b_l(r_c)u^{(\mathrm{irr})'}_{k,l}(r_c)}{a_l(r_c)u^{(\mathrm{reg})}_{k,l}(r_c)+b_l(r_c)u^{(\mathrm{irr})}_{k,l}(r_c)}-\frac{l+1}{r_c}. \quad (13)$$

From this expression it can be checked that if we want the effect of the delta function to be nontrivial, we need $C_0(r_c)$ to be a running coupling constant. In fact, for a constant value of C_0 one finds in the $r_c\to 0$ limit that

$$\frac{b_l(r_c)}{a_l(r_c)}\to-\frac{u^{(\mathrm{reg})}_{k,l}(r_c)}{u^{(\mathrm{irr})}_{k,l}(r_c)}\simeq -r_c^{2l+1}\to 0, \quad (14)$$

meaning that the regular solution is effectively chosen as $|b_l|\ll|a_l|$. Therefore, to avoid a trivial or irrelevant contact interaction one needs that $C_0(r_c)$ evolves with r_c in a very specific way, a dependence that can be obtained by solving Eq. (13) for a given b_l/a_l value.

The running of $C_0(r_c)$ is so strongly determined by the scaling properties of the regular and irregular wave functions near the origin that, if $C_0(r_c)$ is set to be nontrivial in a given partial wave, it will become trivial in all the other waves. This can be checked as follows. If we fit $C_0(r_c)$ to reproduce b_l/a_l in the partial wave $l=l_1$ and call this counterterm $C_0^{(l_1)}(r_c)$, its exact value can be obtained from solving Eq. (13) for $l=l_1$. Using now the counterterm $C_0^{(l_1)}(r_c)$ for computing the linear combination of solutions for $l=l_2(\neq l_1)$, we get the following:

$$\frac{b_{l_2}}{a_{l_2}}\sim r_c^{2l_2+1} \quad \text{for } l_2\neq l_1, \quad (15)$$

which is just the same scaling as the corresponding one for a constant counterterm [Eq. (14)]. Therefore we can take the simplification that a given counterterm only acts on a determined partial wave when the cutoff is removed, as is usually assumed. This means *de facto* a total independence of nontrivial counterterms for any other partial wave. Note that only a trivial counterterm produces a short distance interaction *common* to all partial waves.

B. Delta-shell potentials and attractive singular interactions

As we have seen, to have a nontrivial effect, the running of the counterterm depends on the scaling properties of the wave function near the origin, $r \to 0$. Given the fact that for regular potentials the scaling is different for each partial wave, the result is that only one partial wave will be affected by a given counterterm. On the contrary, as we will see, for attractive singular potentials the scaling does not depend on the angular momentum. Therefore, the scaling is independent of the partial wave chosen, and a given counterterm will affect all the partial waves simultaneously. This is our key observation, which we will extend to tensor forces in Sec. III and put forward below for the relevant case of TPE chiral NN interactions with Δ excitations in Sec. IV.

Indeed, if we consider the behavior of the reduced wave function for a power-law attractive singular potential, which for short enough distances behaves as

$$2\mu V_F(r) \to -\frac{R_F^{n-2}}{r^n}, \tag{16}$$

where $n > 2$ and R_F is some given length scale that sets the range of the power-law behavior of V_F. This new scale R_F may not coincide with the generic range a_F of the potential as several lower energy scales may be present in the system.[6] For a potential like the previous one and for distances $r_c < r \ll R_F$, the reduced wave function can be described by the WKB approximation because the de Broglie wavelength is slowly varying,

$$R_F \frac{d}{dr}\frac{1}{\sqrt{2\mu(E - V_F(r))}} \sim \frac{n}{2}(r/R_F)^{n/2-1} \ll 1, \tag{17}$$

yielding the short distance behavior,

$$u_{k,l}(r) \simeq A_l \left(\frac{r}{R_F}\right)^{n/4} \sin\left[\frac{2}{n-2}\left(\frac{R_F}{r}\right)^{n/2-1} + \varphi_l(k)\right], \quad \text{for } R_F \gg r > r_c, \tag{18}$$

where A_l is some normalization constant and $\varphi_l(k)$ is a short distance phase that in principle depends on the angular momentum and the energy. For $r < r_c$, the reduced wave function $u_{k,l}$ will show the expected r^{l+1} behavior [see Eq. (9)].

Taking into account the behavior of the wave function around the cutoff, we can rewrite the equation that describes the running of C_0 for the case of singular interactions as

$$\frac{2\mu C_0(r_c)}{4\pi r_c^2} = -\frac{2}{R}\left(\frac{R_F}{r_c}\right)^{n/2} \cot\left[\frac{2}{n-2}\left(\frac{R_F}{r_c}\right)^{n/2-1} + \varphi_l(k)\right] - \frac{l+1}{r_c}. \tag{19}$$

As can be immediately realized, for $r_c \to 0$ the explicit l-dependent term stemming from the behavior of the wave function for $r < r_c$ can be dropped, leading to the following ultraviolet behavior for C_0:

$$\frac{2\mu C_0(r_c)}{4\pi r_c^2} \to -\frac{2}{R_F}\left(\frac{R}{r_c}\right)^{n/2} \cot\left[\frac{2}{n-2}\left(\frac{R_F}{r_c}\right)^{n/2-1} + \varphi_l(k)\right], \tag{20}$$

which *does not depend explicitly on angular momentum*. In particular, the previous equation means that for $r_c \to 0$ we have the following identifications:

$$\varphi_l(k_1) = \varphi_l(k_2) \quad \text{and} \quad \varphi_{l_1}(k) = \varphi_{l_2}(k). \tag{21}$$

In other words, the short distance phase is independent of angular momentum or energy. In the more general case that we accept energy-dependent counterterms C_k or higher derivatives of the delta, we can obtain an energy-dependent semiclassical phase $\varphi_l(k_1) \neq \varphi_l(k_2)$, but the angular momentum independence will hold.[7] The only way in which one can break the condition $\varphi_{l_1}(k) = \varphi_{l_2}(k)$ is by accepting terms explicitly depending on the angular momentum in the contact range interaction.

The previous results can be efficiently cast in the language of short distance boundary conditions as follows:

$$\left.\frac{u'_{k,l_1}}{u_{k,l_1}}\right|_{r=r_c+\epsilon} = \left.\frac{u'_{k,l_2}}{u_{k,l_2}}\right|_{r=r_c+\epsilon}, \tag{22}$$

that is, the logarithmic derivative at the cutoff radius of the reduced wave function does not depend on the angular momentum. This is the form in which we will effectively implement the condition $\varphi_{l_1}(k) = \varphi_{l_2}(k)$.

It is important to notice that the angular momentum independence of the behavior of the l wave reduced wave function near the origin is only realized when the cutoff is small enough, so the behavior described in Eq. (18) is valid. In general, Eq. (18) will be applicable for a radius such that the WKB approximation holds, and this radius will be smaller for higher partial waves. If we denote the previous radius as $r_l^{\rm WKB}$, we will generally have $r_{l_1}^{\rm WKB} > r_{l_2}^{\rm WKB}$ for $l_1 < l_2$. This means that for a given cutoff radius there will be a critical value of the angular momentum for which $r_{l_c}^{\rm WKB} > r_c$, and therefore the condition of angular momentum independence should only be used for $l < l_c$, that is,

$$\left.\frac{u'_{k,0}}{u_{k,0}}\right|_{r=r_c+\epsilon} = \left.\frac{u'_{k,1}}{u_{k,1}}\right|_{r=r_c+\epsilon} = \cdots = \left.\frac{u'_{k,l_c-1}}{u_{k,l_c-1}}\right|_{r=r_c+\epsilon}, \tag{23}$$

whereas for higher angular momenta the behavior of the reduced wave function roughly corresponds to what is to be expected for a regular potential, and it may be possible to make a perturbative treatment[8] as suggested in Refs. [37,57].

[6] Actually in the chiral NN potential this is mostly the case where $a_F \sim 1/m_\pi$ and $R_F \sim 1/f_\pi$.

[7] The nth derivative of the delta-function potential generates a discontinuity on the $(n+1)$th derivative of the wave function. As long as the behavior of the wave function is given by Eq. (18), its $(n+1)$th derivative will be angular momentum independent.

[8] The ultraviolet or WKB behavior described by Eq. (18) sets in once there is a deeply bound state in the system, or equivalently, once the zero-energy wave function has reached its first zero (the finite energy wave function will contain anyway zeros from the $\sin(kr + \delta_l - l\pi/2)$ behavior at large distances). This means that for

III. THE INCLUSION OF THE TENSOR FORCE

The previous analysis about the connection between the short-range physics in different partial waves is only valid for the uncoupled channel case. If a tensor force is present, as in the nucleon-nucleon interaction, we will need to account for the induced coupled channel structure happening in spin triplet channels in our analysis. For simplicity, we will assume a two-body system in which the finite range piece of the potential only contains a nontensor (central) and a tensor piece:

$$V_F(\vec{r}) = V_{NT}(r) + S_{12}(\hat{r})V_T(r), \tag{24}$$

with $S_{12}(\hat{r}) = 3\vec{\sigma}_1 \cdot \hat{r}\vec{\sigma}_2 \cdot \hat{r} - \vec{\sigma}_1 \cdot \vec{\sigma}_2$ ($\vec{\sigma}_1$ and $\vec{\sigma}_2$ are the spin operators of particle 1 and 2), and where we do not specify any additional operator structure of the tensor and nontensor pieces of the potential (like, for example, spin or isospin dependence). The behavior of the nontensor and tensor piece at short enough distances is given by

$$V_{NT}(r) \to \frac{C_{NT}}{r^n}, \tag{25}$$

$$V_T(r) \to \frac{C_T}{r^n}, \tag{26}$$

where we have assumed that they have the same power-law divergent behavior at short distances. We have not yet determined whether the potentials are attractive or repulsive.

The tensor force will couple spin triplet channels for which $l = j \pm 1$, being the corresponding reduced Schrödinger equation for $r > r_c$,

$$-u_j'' + U_{11}u_j + U_{12}w_j = k^2 u_j, \tag{27}$$

$$-w_j'' + U_{12}u_j + U_{22}w_j = k^2 w_j, \tag{28}$$

where

$$U_{11} = 2\mu V_{NT} - 2\mu\frac{2j-2}{2j+1}V_T + \frac{j(j-1)}{r^2}, \tag{29}$$

$$U_{12} = 6\frac{\sqrt{j(j+1)}}{2j+1}, \tag{30}$$

$$U_{22} = 2\mu V_{NT} - 2\mu\frac{2j+4}{2j+1}V_T + \frac{(j+1)(j+2)}{r^2}. \tag{31}$$

The previous Schrödinger equation has four linearly independent solutions, of which only two of them are regular and therefore physically acceptable. The coupled channel equations can be efficiently cast into the following compact notation:

$$-\mathbf{u}'' + \left[2\mu\mathbf{V} + \frac{\mathbf{L}^2}{r^2}\right]\mathbf{u} = k^2\mathbf{u}, \tag{32}$$

where the wave function is now a matrix,

$$\mathbf{u} = \begin{pmatrix} u_j^{(a)} & u_j^{(b)} \\ w_j^{(a)} & w_j^{(b)} \end{pmatrix}, \tag{33}$$

with the $^{(a)}$ and $^{(b)}$ superscripts representing the two linearly independent asymptotic ($r \to \infty$) solutions of the system, and where the potential and the angular momentum operator are also 2×2 matrices,

$$\mathbf{V} = \mathbf{1}V_{NT}(r) + \mathbf{S}_{12}^j V_T(r), \tag{34}$$

$$\mathbf{L}^2 = \begin{pmatrix} j(j-1) & 0 \\ 0 & (j+1)(j+2) \end{pmatrix}. \tag{35}$$

In the previous definition of the potential in matrix form, $\mathbf{1}$ represents the identity and $\mathbf{S}_{12}^j$ the tensor operator, that is,

$$\mathbf{1} = \begin{pmatrix} 1 & 0 \\ 0 & 1 \end{pmatrix}, \tag{36}$$

$$\mathbf{S}_{12}^j = \frac{1}{2j+1}\begin{pmatrix} -2(j-1) & 6\sqrt{j(j+1)} \\ 6\sqrt{j(j+1)} & -2(j+2) \end{pmatrix}. \tag{37}$$

The tensor operator can be diagonalized with the following rotation:

$$\mathbf{R}_j = \frac{1}{\sqrt{2j+1}}\begin{pmatrix} \sqrt{j+1} & \sqrt{j} \\ -\sqrt{j} & \sqrt{j+1} \end{pmatrix}, \tag{38}$$

leading to

$$\mathbf{S}_{12,\mathrm{D}}^j = \mathbf{R}_j\mathbf{S}_{12}^j\mathbf{R}_j^{\mathrm{T}} = \begin{pmatrix} 2 & 0 \\ 0 & -4 \end{pmatrix}, \tag{39}$$

$$\mathbf{L}_{j,\mathrm{D}}^2 = \mathbf{R}_j\mathbf{L}^2\mathbf{R}_j^{\mathrm{T}} = \begin{pmatrix} j(j+1) & 2\sqrt{j(j+1)} \\ 2\sqrt{j(j+1)} & j(j+1)+2 \end{pmatrix}, \tag{40}$$

where the $_{\mathrm{D}}$ subscript indicates that the corresponding quantities are defined in the *diagonal* basis. In this basis, the reduced Schrödinger equation is written in the following way:

$$-\mathbf{v}_j'' + 2\mu\left[\mathbf{V}_{j,\mathrm{D}} + \frac{\mathbf{L}_{j,\mathrm{D}}^2}{r^2} + \frac{2\mu\mathbf{C}_{\mathrm{D}}(r_c)}{4\pi r_c^2}\delta(r-r_c)\right]\mathbf{v}_j = k^2\mathbf{v}_j, \tag{41}$$

where $\mathbf{v}_j = \mathbf{R}_j\mathbf{u}_j$ is the rotated wave function, $\mathbf{V}_{j,\mathrm{D}} = \mathbf{R}_j\mathbf{V}\mathbf{R}_j^{\mathrm{T}}$ represents the potential in the diagonal basis, and the contact interaction was explicitly introduced. At short enough distances, $\mathbf{V}_{j,\mathrm{D}}$ behaves in the following way:

$$\mathbf{V}_{j,\mathrm{D}}(r) \to \frac{1}{r^n}\begin{pmatrix} C_{NT}+2C_T & 0 \\ 0 & C_{NT}-4C_T \end{pmatrix}, \tag{42}$$

which means that depending on the signs and relative values of the van der Waals coefficients of the nontensor and tensor piece, C_{NT} and C_T, the diagonalized potential may be attractive-attractive, attractive-repulsive, or repulsive-repulsive. Only two of these situations, namely the attractive-attractive and attractive-repulsive case, admit counterterms [36,58], and are therefore of interest from the point of view of renormalization.

A. Attractive-attractive case

Situations where both eigenchannels are attractive are the easiest to handle. If a singular power-law potential is assumed,

radii bigger than r_l^{WKB} or r_l^{bound} the perturbative expansion is expected to converge.

the behavior of the reduced wave function for $r < r_c$ can be safely ignored, yielding the following relation:

$$\mathbf{v}_j{}'(r_c)\mathbf{v}_j(r_c)^{-1} = \frac{2\mu}{4\pi r_c^2}\mathbf{C}_{\rm D}(r_c), \tag{43}$$

meaning that there are three free parameters in this case (because of $\mathbf{C}_{\rm D}$ being real and symmetric), in agreement with previous analysis of singular potentials in coupled channels [36,58]. The relation between the short-range wave functions of channels with different total angular momentum is, therefore,

$$\mathbf{v}^{\rm T}_{j_2}\mathbf{v}'_{j_1} = \mathbf{v}^{\rm T}_{j_2}{}'\mathbf{v}_{j_1}, \tag{44}$$

where we have made use of $\mathbf{C}_{\rm D} = \mathbf{C}^{\rm T}_{\rm D}$. This relation is invariant with respect to the relative normalization of the two linearly independent solutions of each partial wave, which were previously denoted with the $^{(a)}$ and $^{(b)}$ superscripts, and also on the set of linearly independent solutions chosen, as can be easily checked. It should be noted, too, that the previous relation is reminiscent of the coupled-channel version of the two-potential formula of Ref. [59].

A problem arises in relating the $j = 0$ triplet state with other coupled channels, as the $^3P_0$ wave is effectively an uncoupled state,

$$\mathbf{v}_{j=0}(r) = \begin{pmatrix} 0 & 0 \\ 0 & v_{^3P_0}(r) \end{pmatrix}. \tag{45}$$

Therefore, the previous representation of the short distance potential [i.e., the coupled-channel delta shell of Eq. (43)], cannot be a correct representation of the short-range physics of the $^3P_0$ channel. As a consequence the $^3P_0$ channel cannot be *unambiguously* related with the other coupled channels. It is possible, however, to obtain convergent amplitudes by relating the $^3P_0$ wave function with any of the "lower" *eigen* wave functions of the reference wave function $\mathbf{v}_j$,

$$\frac{v'_{^3P_0}(r_c)}{v_{^3P_0}(r_c)} = \frac{(\mathbf{v}_j)'_{21}(r_c)}{(\mathbf{v}_j)_{21}(r_c)} \quad \text{or} \quad \frac{v'_{^3P_0}(r_c)}{v_{^3P_0}(r_c)} = \frac{(\mathbf{v}_j)'_{22}(r_c)}{(\mathbf{v}_j)_{22}(r_c)}, \tag{46}$$

where $_{21}$ and $_{22}$ are the corresponding indices in the rotated wave function matrix v_2. Both possibilities yield a renormalizable phase for the $^3P_0$ wave, but not the same one: The phase shift depends on which of the previous two equations is used, indicating the presence of model dependence in any of these choices. Therefore, the only way to avoid model dependence is to treat the $^3P_0$ wave as an independent wave in the attractive-attractive case.

B. Attractive-repulsive case

If one of the eigenchannels is attractive and the other is repulsive, then we have that Eq. (43) can only be applied in the attractive eigenchannel. In particular, the delta-shell coupling matrix $\mathbf{C}_{\rm D}(r_c)$ takes the simplifying form,

$$\mathbf{C}_{\rm D}(r_c)_{BC} = C_A(r_c)\delta_{AB}\delta_{AC}, \tag{47}$$

where the labels $B, C = 1, 2$ are matrix indices, and A represents the index associated with the attractive solution, that is, only one counterterm is needed to renormalize an attractive-repulsive coupled channel, as delta-shell contributions become trivial in the $r_c \to 0$ limit, except if they happen in the AA subchannel. Combining the previous result with the boundary condition induced by the delta-shell potential,

$$\mathbf{v}_j{}'(r_c) = \frac{2\mu}{4\pi r_c^2}\mathbf{C}_{\rm D}(r_c)\mathbf{v}_j(r_c), \tag{48}$$

the following renormalization conditions are obtained:

$$\frac{(\mathbf{v}_{j_1}{}'(r_c))_{AA}}{(\mathbf{v}_{j_1}(r_c))_{AA}} = \frac{(\mathbf{v}_{j_2}{}'(r_c))_{AA}}{(\mathbf{v}_{j_2}(r_c))_{AA}}, \tag{49}$$

$$\frac{(\mathbf{v}_{j_1}{}'(r_c))_{AR}}{(\mathbf{v}_{j_1}(r_c))_{AR}} = \frac{(\mathbf{v}_{j_2}{}'(r_c))_{AR}}{(\mathbf{v}_{j_2}(r_c))_{AR}}, \tag{50}$$

$$(\mathbf{v}_{j_1}{}'(r_c))_{RA} = (\mathbf{v}_{j_2}{}'(r_c))_{RA} = 0, \tag{51}$$

$$(\mathbf{v}_{j_1}{}'(r_c))_{RR} = (\mathbf{v}_{j_2}{}'(r_c))_{RR} = 0, \tag{52}$$

where R is the index of the repulsive eigenchannel. The first two equations relate the attractive eigenchannels of different partial waves, although they are redundant. From the form of the delta-shell coupling matrix $\mathbf{C}_{\rm D}(r_c)$, together with Eq. (48), one obtains that

$$\frac{(\mathbf{v}_j{}'(r_c))_{AA}}{(\mathbf{v}_j(r_c))_{AA}} = \frac{(\mathbf{v}_j{}'(r_c))_{AR}}{(\mathbf{v}_j(r_c))_{AR}}, \tag{53}$$

implying the equivalence of Eqs. (49) and (50). The last two equations [Eqs. (51) and (52)], are just regularization conditions for the repulsive eigenchannels. Contrary to what happened in the attractive-attractive case, in the attractive-repulsive case the $j = 0$ $^3P_0$ wave (if attractive) can be directly related with the other coupled triplet waves.

IV. APPLICATION TO NEUTRON-PROTON SCATTERING

The previous results can be applied to the case neutron-proton (np) scattering in nuclear effective field theory, where the resulting potentials are in many cases singular and attractive. In principle, we can relate any two partial waves for which the potential diverges in the same way (i.e., the *same* power and the *same* coefficient). This means that correlations will emerge only between channels with the same spin and isospin values. For the spin triplet channels it is also necessary to consider whether the channels are coupled ($l = j \pm 1$) or uncoupled ($l = j$). Therefore, we obtain a total of six sets of correlated waves, namely (i) singlet isovectors, (ii) singlet isoscalars, (iii) uncoupled triplet isovectors, (iv) uncoupled triplet isoscalars, (v) coupled triplet isovectors, and (vi) coupled triplet isoscalars. We limit ourselves to the $j \leqslant 5$ partial waves. The $^3P_0$ wave remains uncorrelated in our current scheme and it is not further considered in this work.

A. The chiral neutron-proton potential

The finite range piece of the nucleon-nucleon (NN) potential in chiral perturbation theory is expressed as an expansion in powers of Q,

$$V_{NN}(\vec{r}) = V_\chi^{(0)}(\vec{r}) + V_\chi^{(2)}(\vec{r}) + V_\chi^{(3)}(\vec{r}) + \mathcal{O}(Q^4), \tag{54}$$

where Q represents either the pion mass, the nucleon-Δ splitting, or the momentum of the nucleons. We only consider here chiral potentials in which the Δ isobar was explicitly included [17,53]. The reasons for this decision are that (i) they have better convergence properties than their Δ-less counterparts, and (ii) they are attractive-attractive singular interactions in all coupled channels at orders Q^2 (NLO) and Q^3 (N^{2}LO), leading to a simpler analysis in general. For the finite range piece of the interaction we adopt the original Weinberg counting [10], in which $1/M_N$ corrections are treated as higher order as it is done in Refs. [15,60,61]. At the orders considered in this work, the potential can be decomposed as a central, spin-spin, and a tensor component, which in coordinate space reads

$$V_{NN}(\vec{r}) = V_C(r) + \tau W_C(r) + \sigma(V_S(r) + \tau W_S(r)) + S_{12}(\hat{r})(V_T(r) + \tau W_T(r)), \quad (55)$$

where spin-orbit and quadratic spin-orbit terms have been ignored as they do not appear up to higher orders. The use of previous counting rule for the $1/M_N$ corrections is necessary if we plan to correlate at short distance the behavior of the different waves, as it generates a spin-orbit term that is less singular than the other components of the interaction. The operators τ, σ, and S_{12} are given by

$$\begin{aligned} \tau &= \vec{\tau}_1 \cdot \vec{\tau}_2 = 2t(t+1) - 3, \\ \sigma &= \vec{\sigma}_1 \cdot \vec{\sigma}_2 = 2s(s+1) - 3, \\ S_{12}(\hat{r}) &= 3\vec{\sigma}_1 \cdot \hat{r}\vec{\sigma}_2 \cdot \hat{r} - \vec{\sigma}_1 \cdot \vec{\sigma}_2, \end{aligned} \quad (56)$$

where $\vec{\tau}_{1(2)}$ and $\vec{\sigma}_{1(2)}$ are the proton(neutron) isospin and spin operators; t and s represent the total isospin $t = 0, 1$ and total spin $s = 0, 1$ of the np system. The precise form of the chiral Δ potential is taken from Ref. [53].

Note that in the singlet channel cases ($s = 0$) the tensor force operator does not contribute. For symmetry reasons (Fermi-Dirac statistics) we have $(-)^{l+s+t} = -1$, where l is the orbital angular momentum. This means in particular that even partial waves are isovectors ($t = 1$) and odd partial waves are isoscalars ($t = 0$). The NN potential reads for the singlet channels,

$$\begin{aligned} V_{^1S_0}(r) &= V_{^1D_2}(r) = V_{^1G_4}(r) \\ &= V_C(r) + W_C(r) - 3V_S(r) - 3W_S(r), \\ V_{^1P_1}(r) &= V_{^1F_3}(r) = V_{^1H_5}(r) \\ &= V_C(r) - 3W_C(r) - 3V_S(r) + 9W_S(r), \end{aligned} \quad (57)$$

that is, all the singlet channels can be described with two different potentials depending on whether we are in the isoscalar or isovector case (or equivalently, on whether even or odd partial waves are considered).

In the spin triplet channels ($s = 1$) we must distinguish between uncoupled ($l = j$) and coupled waves ($l = j \pm 1$). In the uncoupled waves, we can again distinguish between the potential in the isoscalar ($^3D_2$, $^3G_4$) and isovector ($^3P_1$, $^3D_2$) waves:

$$V_{^3D_2}(r) = V_{^3G_4}(r), \quad V_{^3P_1}(r) = V_{^3F_3}(r) = V_{^3H_5}(r), \quad (58)$$

where the explicit expressions of the previous potentials in terms of the central, spin-spin, and spin-tensor components is given by

$$\begin{aligned} V_{^3D_2}(r) &= V_C(r) - 3W_C(r) + V_S(r) - 3W_S(r) \\ &\quad + 2V_T(r) - 6W_T(r), \quad (59) \\ V_{^3P_1}(r) &= V_C(r) + W_C(r) + V_S(r) + W_S(r) \\ &\quad + 2V_T(r) + 2W_T(r). \quad (60) \end{aligned}$$

Equivalently, for the coupled waves we have

$$\begin{aligned} \mathbf{R}_1 \mathbf{V}_{^3C_1}(r) \mathbf{R}_1^{\mathrm{T}} &= \mathbf{R}_3 \mathbf{V}_{^3C_3}(r) \mathbf{R}_3^{\mathrm{T}} = \mathbf{R}_5 \mathbf{V}_{^3C_5}(r) \mathbf{R}_5^{\mathrm{T}}, \\ \mathbf{R}_2 \mathbf{V}_{^3C_2}(r) \mathbf{R}_2^{\mathrm{T}} &= \mathbf{R}_4 \mathbf{V}_{^3C_4}(r) \mathbf{R}_4^{\mathrm{T}}, \end{aligned} \quad (61)$$

for the isoscalar ($^3C_1$, $^3C_3$, $^3C_5$) and isovector ($^3C_2$, $^3C_4$) waves, and where the expressions are more cumbersome as they involve matrices. In the expressions above, $\mathbf{R}_j$ are the rotation matrices defined in Eq. (38). The notation $^3C_1$, $^3C_2$, etc., is a short hand for $^3S_1 - {}^3D_1$, $^3P_2 - {}^3F_2$, etc., and the explicit form of the rotated potentials is given by

$$\begin{aligned} \mathbf{R}_1 \mathbf{V}_{^3C_1}(r) \mathbf{R}_1^{\mathrm{T}} &= \mathbf{1}(V_C(r) - 3W_C(r) + V_S(r) - 3W_S(r)) \\ &\quad + \mathbf{S}^j_{12,\mathrm{D}}(V_T(r) - 3W_T(r)), \\ \mathbf{R}_2 \mathbf{V}_{^3C_2}(r) \mathbf{R}_2^{\mathrm{T}} &= \mathbf{1}(V_C(r) + W_C(r) + V_S(r) + W_S(r)) \\ &\quad + \mathbf{S}^j_{12,\mathrm{D}}(V_T(r) + W_T(r)), \end{aligned} \quad (62)$$

with $\mathbf{1}$ the 2×2 identity matrix, and $\mathbf{S}^j_{12,\mathrm{D}}$ the diagonalized tensor matrix represented by Eq. (39).

B. Van der Waals behavior of the chiral potentials

At distances below the pion Compton wavelength, $m_\pi r \ll 1$, the chiral potentials exhibit at orders Q^2 and Q^3 a power-law behavior of the type,

$$V^{(\nu)}(r) \to \frac{C_6^{(\nu)}}{r^6}, \quad (63)$$

with $\nu = 2, 3$ and where the value of $C_6^{(\nu)}$ depends on the particular component of the potential considered. These coefficients were computed in Ref. [52] based on the spectral function representation of the potentials of Krebs, Epelbaum, and Meißner [53]. It should be noted though that the exact behavior of the potential at short distances is inessential for the angular momentum correlations. What really matters is (i) that the potential is a singular attractive interaction and (ii) that it is much stronger than the centrifugal barrier at the chosen cutoff radius r_c. In the case of the order Q^2 and Q^3 chiral Δ-full potentials these conditions are fulfilled in all partial waves with $j \leqslant 5$ for cutoff radii as big as 1.0 fm.

C. Correlated renormalization of the uncoupled waves

We describe the scattering states in the uncoupled waves by solving the following reduced Schrödinger equation for $r > r_c$:

$$-u''_{k,l} + \left[M_N V_{NN}(r) + \frac{l(l+1)}{r^2} \right] u_{k,l}(r) = k^2 u_{k,l}(r), \quad (64)$$

where $u_{k,l}$ is the reduced wave function, V_{NN} the corresponding chiral potential for the particular partial wave considered, k the center-of-mass momentum, l the angular momentum, and M_N is twice the neutron-proton reduced mass [i.e., $M_N = 2M_pM_n/(M_p + M_n)$]. The reduced wave function is asymptotically normalized to

$$u_{k,l}(r) \to k^l(\cot\delta_l \hat{j}_l(kr) - \hat{y}_l(kr)), \tag{65}$$

for $r \to \infty$, with δ_l the phase shift, and $\hat{j}_l(x) = x j_l(x)$ and $\hat{y}_l(x) = x y_l(x)$ the reduced spherical Bessel functions. The normalization factor k^l is added to have a well-defined normalization of the wave function in the $k \to 0$ limit. At $r = r_c$ the wave function can be determined by several means. One is by solving Eq. (19) for some value of the counterterm C_0, which can be later fitted to reproduce some observable, like, for example, the $^1S_0$ (or $^1P_1/^3P_1/^3D_2$) scattering length. A different way is to construct an asymptotic wave function ($r \to \infty$) reproducing the desired scattering length. In the case of the $^1S_0$ channel, this wave function is given by

$$u_{0,^1S_0}(r) \to 1 - \frac{r}{a_0}, \tag{66}$$

with a_0 the $^1S_0$ scattering length, and then integrate the reduced Schrödinger equation, Eq. (64), downward from $r \to \infty$ to $r = r_c$. Then we use the different relations derived previously to obtain the logarithmic boundary condition at $r = r_c$ for the different energies and partial waves considered. For the particular case of the $^1S_0$ channel and its correlated channels $^1D_2$ and $^1G_4$, the relation takes the form,

$$\left.\frac{u'_{0,^1S_0}}{u_{0,^1S_0}}\right|_{r=r_c} = \left.\frac{u'_{k,^1S_0}}{u_{k,^1S_0}}\right|_{r=r_c}, \tag{67}$$

$$\left.\frac{u'_{k,^1S_0}}{u_{k,^1S_0}}\right|_{r=r_c} = \left.\frac{u'_{k,^1D_2}}{u_{k,^1D_2}}\right|_{r=r_c} = \left.\frac{u'_{k,^1G_4}}{u_{k,^1G_4}}\right|_{r=r_c}, \tag{68}$$

where the first equation relates the zero and finite energy states of the $^1S_0$ wave, and the second one represents the partial-wave correlations. For the other correlated channels, we have the correlation conditions,

$$\left.\frac{u'_{k,^1P_1}}{u_{k,^1P_1}}\right|_{r=r_c} = \left.\frac{u'_{k,^1F_3}}{u_{k,^1F_3}}\right|_{r=r_c} = \left.\frac{u'_{k,^1H_5}}{u_{k,^1H_5}}\right|_{r=r_c}, \tag{69}$$

$$\left.\frac{u'_{k,^3P_1}}{u_{k,^3P_1}}\right|_{r=r_c} = \left.\frac{u'_{k,^3F_3}}{u_{k,^3F_3}}\right|_{r=r_c} = \left.\frac{u'_{k,^3H_5}}{u_{k,^3H_5}}\right|_{r=r_c}, \tag{70}$$

$$\left.\frac{u'_{k,^3D_2}}{u_{k,^3D_2}}\right|_{r=r_c} = \left.\frac{u'_{k,^3G_4}}{u_{k,^3G_4}}\right|_{r=r_c}, \tag{71}$$

which are to be supplemented with the regularization conditions for the *base* waves,

$$\left.\frac{u'_{0,^1P_1}}{u_{0,^1P_1}}\right|_{r=r_c} = \left.\frac{u'_{k,^1P_1}}{u_{k,^1P_1}}\right|_{r=r_c}, \tag{72}$$

$$\left.\frac{u'_{0,^3P_1}}{u_{0,^3P_1}}\right|_{r=r_c} = \left.\frac{u'_{k,^3P_1}}{u_{k,^3P_1}}\right|_{r=r_c}, \tag{73}$$

$$\left.\frac{u'_{0,^3D_2}}{u_{0,^3D_2}}\right|_{r=r_c} = \left.\frac{u'_{k,^3D_2}}{u_{k,^3D_2}}\right|_{r=r_c}. \tag{74}$$

These boundary conditions can be used as initial integration conditions for the corresponding Schrödinger equation [Eq. (64)]. After integrating upward from $r = r_c$ to $r \to \infty$, we match to the asymptotic behavior of the wave functions [Eq. (66)] to obtain the phase shifts. The equivalent value for the counterterm coupling $C_0(r_c)$ can be obtained from Eq. (19), giving in the $r_c \to 0$ limit,

$$\frac{M_N C_{^1S_0}(r_c)}{4\pi r_c^2} \simeq \frac{u'_{0,^1S_0}(r_c)}{u_{0,^1S_0}(r_c)}, \tag{75}$$

plus the corresponding expressions for the other base waves.

D. Correlated renormalization of the coupled waves

For the coupled channels we solve the coupled reduced Schrödinger equation in its matrix form:

$$-\mathbf{u}_{k,j}{}'' + \left[2\mu \mathbf{V}_{NN}(r) + \frac{\mathbf{L}^2}{r^2}\right]\mathbf{u}_{k,j}(r) = k^2 \mathbf{u}_{k,j}(r), \tag{76}$$

where we now use the notation of Sec. III in which $\mathbf{u}_{k,j}$, $\mathbf{V}_{NN}$, and $\mathbf{L}^2$ are matrices. The reduced wave function is asymptotically ($r \to \infty$) normalized to

$$\mathbf{u}_{k,j} \to (\mathbf{j}_j(kr)\mathbf{M}_j(k) - \mathbf{y}_j(kr))\mathbf{F}_j(k), \tag{77}$$

where $\mathbf{j}_j(kr)$, $\mathbf{y}_j(kr)$, and $\mathbf{F}_j(k)$ are diagonal matrices defined as

$$\mathbf{j}_j(kr) = \begin{pmatrix} \hat{j}_{j-1}(kr) & 0 \\ 0 & \hat{j}_{j+1}(kr) \end{pmatrix}, \tag{78}$$

$$\mathbf{y}_j(kr) = \begin{pmatrix} \hat{y}_{j-1}(kr) & 0 \\ 0 & \hat{y}_{j+1}(kr) \end{pmatrix}, \tag{79}$$

$$\mathbf{F}_j(k) = \begin{pmatrix} k^{j-1} & 0 \\ 0 & k^{j+1} \end{pmatrix}, \tag{80}$$

with $\hat{j}_l(x) = x j_l(x)$ and $\hat{y}_l(x) = x y_l(x)$ the reduced spherical Bessel functions. The normalization factor $\mathbf{F}_j(k)$ is included in order to have a well-defined asymptotic ($r \to \infty$) wave function at $k = 0$. The $\mathbf{M}_j(k)$ matrix is the coupled-channel equivalent of $\cot\delta_l(k)$ and is related to the S matrix $\mathbf{S}_j(k)$ by $\mathbf{M}_j(k) = i(\mathbf{S}_j(k) + \mathbf{1})/(\mathbf{S}_j(k) - \mathbf{1})$ with $\mathbf{1}$ the 2×2 identity matrix.

For the chiral Δ-full potential of Ref. [53] all the coupled channels are attractive-attractive singular potentials at distances below the pion Compton wavelength. Thus three renormalization conditions or counterterms are needed to obtain well-defined results. The usual procedure is to fix the asymptotic ($r \to \infty$) behavior of the wave function at $k = 0$, that is, we fix the three scattering lengths of the coupled system. Then we integrate the Schrödinger equation [Eq. (76)], downward from $r \to \infty$ to $r = r_c$. If we define $\mathbf{L}_{k,j}(r)$ as

$$\mathbf{L}_{k,j}(r) = \mathbf{u}'_{k,j}(r)\mathbf{u}_{k,j}{}^{-1}(r), \tag{81}$$

then the finite energy solution is constructed from the following boundary condition at $r = r_c$,

$$\mathbf{L}_{k,j}(r_c) = \mathbf{L}_{0,j}(r_c). \tag{82}$$

The procedure for correlating the different partial waves considered is similar to the one employed in constructing the finite energy solutions, the only difference being the rotation to the basis in which the tensor force is diagonal. For the two sets of correlated coupled channels, those with $j = 1, 3, 5$ and those with $j = 2, 4$, we have the boundary conditions,

$$\mathbf{R_1}\mathbf{L}_{k,1}(r_c)\mathbf{R_1}^{\mathrm{T}} = \mathbf{R_3}\mathbf{L}_{k,3}(r_c)\mathbf{R_3}^{\mathrm{T}} = \mathbf{R_5}\mathbf{L}_{k,5}(r_c)\mathbf{R_5}^{\mathrm{T}}, \quad (83)$$

$$\mathbf{R_2}\mathbf{L}_{k,2}(r_c)\mathbf{R_2}^{\mathrm{T}} = \mathbf{R_4}\mathbf{L}_{k,4}(r_c)\mathbf{R_4}^{\mathrm{T}}, \quad (84)$$

from which the $\mathbf{M}_{k,j}(k)$ matrix (and the corresponding phase shifts) can be obtained.

E. Cutoff dependence of the phase shifts

The cutoff dependence of the phase shifts in the correlated renormalization procedure can be easily estimated by making use of the renormalization group analysis of boundary condition regularization of Ref. [40]. For simplicity, we only consider in detail the uncoupled channel case. According to Ref. [40], the cutoff dependence of the phase shift for an uncoupled channel is given by

$$\frac{d\delta_l(k;r_c)}{dr_c} = \Big[M_N V_{NN}(r_c) - k^2 + \frac{l(l+1)}{r_c^2} + L'_{k,l}(r_c) + L^2_{k,l}(r_c)\Big] u^2_{k,l}(r_c), \quad (85)$$

where $\delta_l(k)$ is the phase shift, r_c the cutoff radius, and with $u_{k,l}$, V_{NN}, k, l, and M_N as defined in Eq. (64). In the previous formula $L_{k,l}(r_c)$ is the logarithmic derivative of the $u_{k,l}$ reduced wave function at the cutoff radius, that is,

$$L_{k,l}(r_c) = \frac{u'_{k,l}(r_c)}{u_{k,l}(r_c)}. \quad (86)$$

If we are correlating the l_0 and l waves, we have for the logarithmic derivatives at the cutoff radius r_c that

$$L_{k_0,l_0}(r_c) = L_{k,l}(r_c), \quad (87)$$

where the partial wave l_0 is taken to be the *base* wave, that is, the wave for which we have fixed the value of the phase shift at $k = k_0$ (or the scattering length if $k_0 = 0$). By taking into account that the reduced wave function $u_{k_0,l_0}(r)$ obeys the following Schrödinger equation,

$$-u''_{k_0,l_0}(r) + \left[M_N V_{NN}(r) + \frac{l_0(l_0+1)}{r^2}\right] u_{k_0,l_0}(r) = k_0^2 u_{k_0,l_0}(r), \quad (88)$$

it is trivial to check that the logarithmic boundary condition for $k = k_0$, $l = l_0$ fulfills the differential equation,

$$M_N V_{NN}(r_c) + \frac{l_0(l_0+1)}{r_c^2} - k_0^2 + L'_{k_0,l_0}(r_c) + L^2_{k_0,l_0}(r_c) = 0, \quad (89)$$

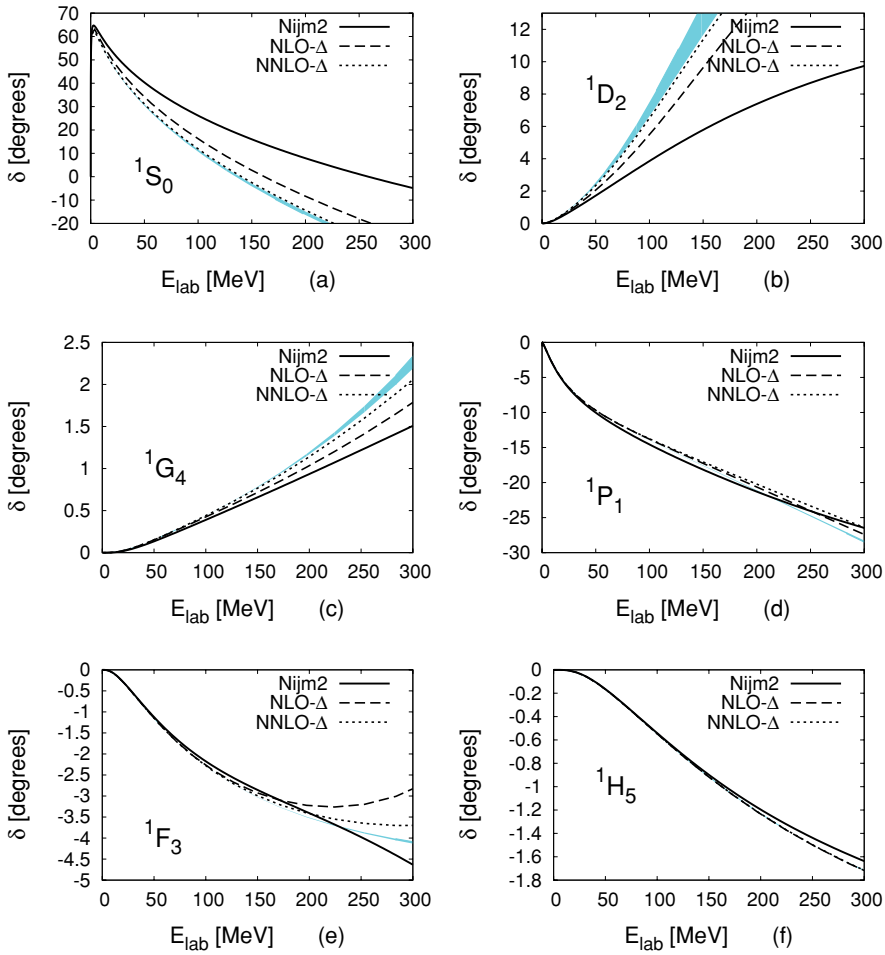

FIG. 1. (Color online) (Panels a, b and c) $^1S_0$, $^1D_2$, and $^1G_4$ phase shifts computed from Eq. (67), using the $^1S_0$ scattering length as an input parameter with a coordinate space cutoff $r_c = 0.3$ fm. (Panels d, e and f) $^1P_1$, $^1F_3$, and $^1H_5$ phase shifts computed from Eq. (69), using the $^1P_1$ scattering length as an input parameter with a coordinate space cutoff $r_c = 0.3$ fm. The light blue band is generated by varying the cutoff radius within the range $r_c = 0.6 - 0.8$ fm.

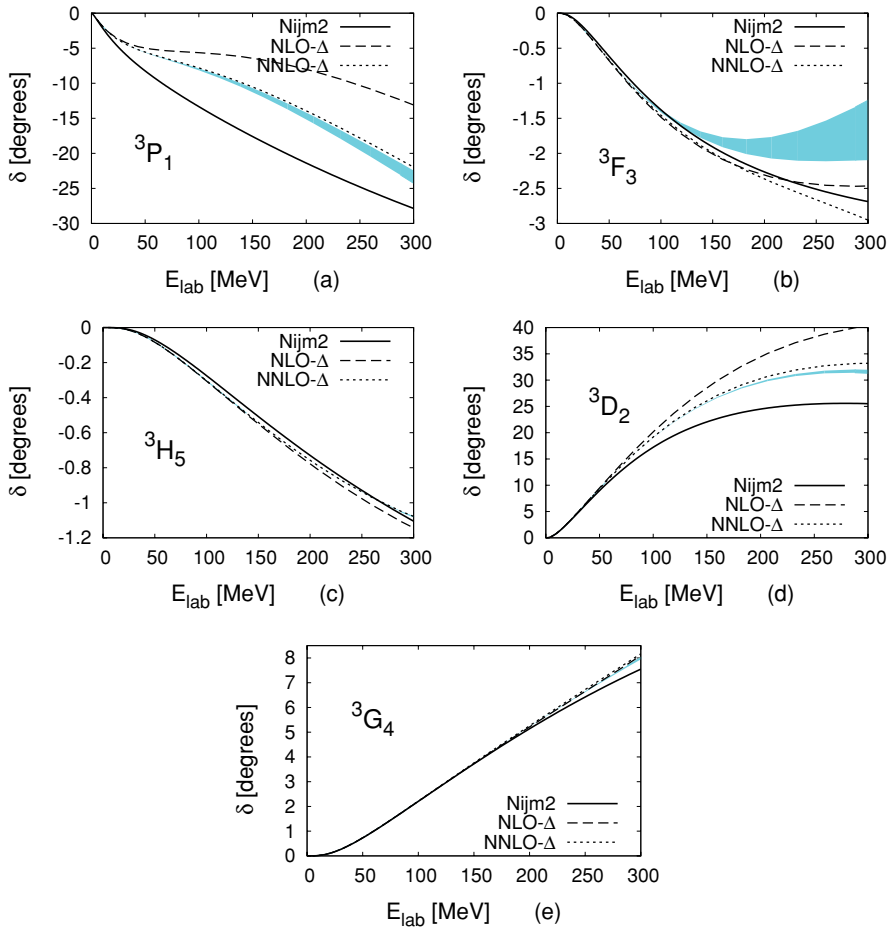

FIG. 2. (Color online) (Panels a, b and c) $^3P_1$, $^3F_3$, and $^3H_5$ phase shifts computed from Eq. (70), using the $^3P_1$ scattering length as an input parameter with a coordinate space cutoff $r_c = 0.3$ fm. (Panels d and e) $^3D_2$ and $^3G_4$ phase shifts computed from Eq. (71), using the $^3D_2$ scattering length as an input parameter with a coordinate space cutoff $r_c = 0.3$ fm. The light blue band is generated by varying the cutoff radius within the range $r_c = 0.6$–0.8 fm.

which is also the differential equation obeyed by $L_{k,l}(r_c)$. In particular, the previous means that the cutoff dependence of the phase shift simplifies to

$$\frac{d\delta_l(k;r_c)}{dr_c} = \left[\frac{l(l+1)-l_0(l_0+1)}{r_c^2} - \left(k^2-k_0^2\right)\right]u_{k,l}^2(r_c). \tag{90}$$

For cutoff radii such that $2m_\pi r_c \ll 1$, the behavior of the wave functions will be determined by the van der Waals piece of the interaction [i.e., $u_{k,l}^2(r_c) \sim r_c^3$], up to oscillations [see Eq. (18)] for the chiral NLO- and N^{2}LO-Δ potentials of Ref. [53]. This implies that the cutoff dependence of the phase shifts can be approximated by

$$\delta_{l_0}(k,r_c) - \delta_{l_0}(k,0) \propto -\left(k^2-k_0^2\right)r_c^4, \tag{91}$$

for $l = l_0$ (that is, the *base* wave), and

$$\delta_l(k,r_c) - \delta_l(k,0) \propto [l(l+1)-l_0(l_0+1)]r_c^2, \tag{92}$$

for $l \neq l_0$. At the end of Sec. V, we illustrate these expectations for the chiral Δ potentials of Ref. [53]. It should be noted that Eq. (90) implies that the correlated renormalization procedure only generates converging phase shifts if the potential V_{NN} is singular, as expected from the discussion in Sec. II. The extension of the previous results to coupled channels is straightforward and leads to the same conclusion and cutoff dependence as the uncoupled channel case.

V. NUMERICAL RESULTS

As we have shown we can relate the phase shifts in different partial waves using the short-range relation described by Eqs. (67)–(71). We take in our numerical computations $f_\pi = 92.4$ MeV, $m_\pi = 138.03$ MeV, $2\mu_{np} = M_N = 2M_pM_n/(M_p+M_n) = 938.918$ MeV, $g_A = 1.29$ in the OPE piece to account for the Goldberger-Treimann discrepancy and $g_A = 1.26$ in the TPE piece of the potential. The discussion of the standard OPE potential corresponds to the attractive-repulsive case and is relegated to Appendix A. We discuss here the TPE chiral potential with Δ excitations as obtained from Ref. [53] (however with the spectral cutoff removed). For h_A, the chiral couplings c_1, c_3, and c_4, and $\tilde{b} = b_3 + b_8$ we take the values corresponding to "Fit 1" of Ref. [53] (see Table I inside the previous reference).

All the partial waves are renormalized at a cutoff radius $r_c = 0.3$ fm. This cutoff is small enough by far: In most partial waves the phase shifts have already converged in the range $r_c = 0.6$–0.8 fm. Smaller cutoff radii are in principle possible, but require too much computing time for the higher partial waves, whereas cutoff radii larger than 0.8- to 1.0-fm yield amplitudes, which depend linearly on the cutoff for low partial waves. The appearance of the first deeply bound state usually happens in the 0.5- to 1.0-fm region, the exact location depending on the particular partial wave considered. Even in the case of G and H waves there are usually between two and three

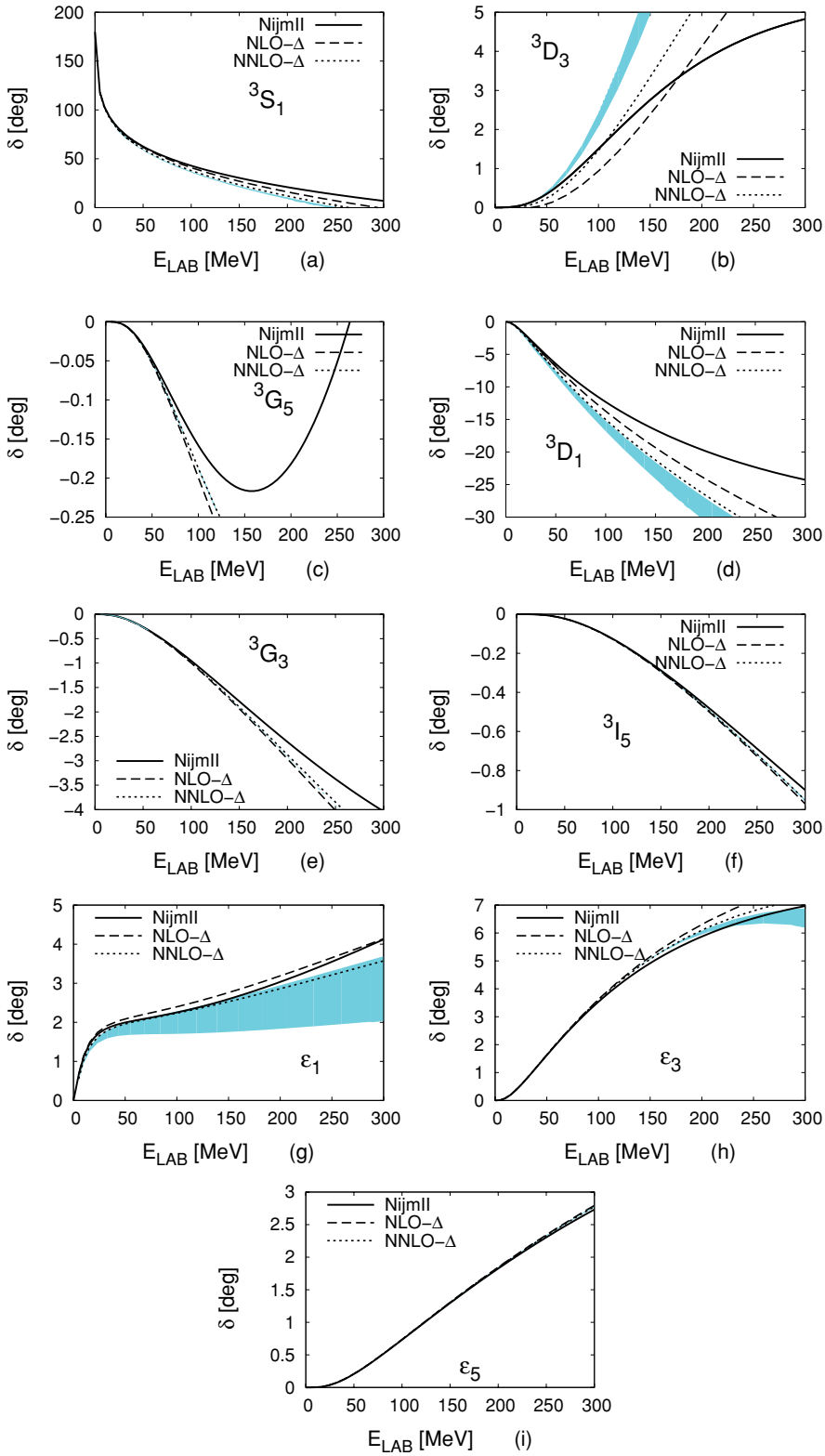

FIG. 3. (Color online) $^3S_1$-$^3D_1$, $^3D_3$-$^3G_3$, and $^3G_5$-$^3I_5$ coupled channel phase shifts. The $^3S_1$-$^3D_1$ wave is computed from orthogonality to the deuteron bound state and from the triplet scattering length $a_{0,t} = 5.419$ fm. The $^3D_3 - {}^3G_3$ and $^3G_5 - {}^3I_5$ coupled channels are computed from the partial-wave correlation given by Eq. (83) *without* introducing new counterterms. We use the same cut-off values as in Figs. (1) and (2).

deeply bound states at $r_c = 0.3$ fm. At these distances the wave functions are dominated by the van der Waals behavior of the NLO-Δ and N^{2}LO-Δ potentials, meaning that the correlated renormalization procedure is guaranteed to work. This does not imply, however, that the low-energy phase shifts are dominated by the singular structure of the chiral potentials at distances below the pion Compton wavelength. In fact, as will be commented in the following paragraphs, the results for peripheral waves do not significantly differ from those computed in first-order perturbation theory [53]. The explicit cutoff dependence of the phase shifts is discussed in more detail for selected partial waves at the end of this section.

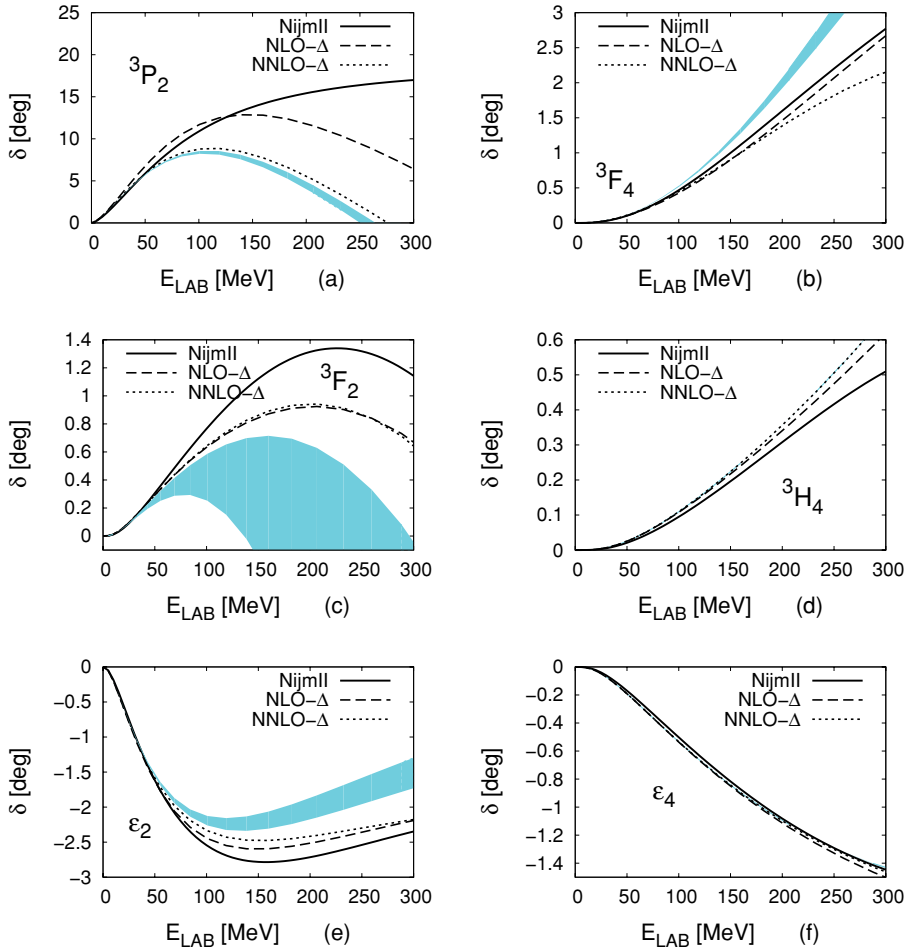

FIG. 4. (Color online) $^3P_2$-$^3F_2$ and $^3F_4$-$^3H_4$ phase shifts. The $^3P_2$-$^3F_2$ wave is constructed to reproduce the Nijmegen II scattering lengths for this coupled channel, whereas the $^3F_4$-$^3H_4$ wave is obtained from the partial-wave correlation described in Eq. (84) *without* introducing new counterterms. The values of the coordinate space cutoffs are the same as in Figs. 1 and 2.

In Fig. 1, we show the results for the singlet waves. For the $^1S_0$-$^1D_2$-$^1G_4$ ($^1P_1$-$^1F_3$-$^1H_5$) correlation we have taken as input parameter the $^1S_0$ ($^1P_1$) scattering length from the Nijmegen II potential [5], which was computed in Ref. [62] yielding the result $a_{^1S_0} = -23.727$ fm ($a_{^1P_1} = 2.797\,\text{fm}^3$). For the $^1G_4$ phase in the isovector channels and the $^1F_3$ wave in the isosinglet, the phase shifts do not differ much from those obtained in Ref. [53] in the Born approximation (in the previous reference only waves with $l = 2, 3, 4$ were considered). The $^1H_5$ is also very similar to the phases obtained in Refs. [16,17] for the NLO-Δ potential. These waves are also quite similar to those obtained in Ref. [36] by renormalizing the N^{2}LO potential for the Δ-less theory in a wave-by-wave basis, that is, by fixing the scattering lengths separately in each of the channels to their Nijmegen II values. In general, peripheral partial waves will not notice too much the inclusion of the two-pion exchange interaction or the Δ excitation and will behave very similarly as in first-order perturbation theory. In this regard, the partial-wave correlation is useful mainly as a way to renormalize all the peripheral waves with a minimum number of counterterms, but not necessarily as a real correlation. The only wave in which it can be effectively noticed is in the $^1D_2$ one, in which the $^1S_0$-$^1D_2$ correlation predicts a scattering length of $a_{^1D_2} = -1.728$ fm^5 for the $^1D_2$ wave,[9] to be compared with an optimal scattering length of $a_{^1D_2} = -1.686$ fm^5 for which the N^{2}LO-Δ potential effectively reproduces the Nijmegen II results for $E_{\text{LAB}} \leqslant 150$ MeV. The previous observation indicates the necessity of the specific $^1D_2$ wave N^{3}LO counterterm to reproduce the results in this partial wave. The predicted value greatly differs from the one corresponding to the Nijmegen II or Reid93 potentials [5], namely $a_{^1D_2,\text{Nijm2}} = -1.389$ fm^5 and $a_{^1D_2,\text{Reid93}} = -1.377$ fm^5, which were computed in Ref. [62]. This discrepancy is, however, common in most effective field theory computations in which the scattering length is fixed (see, for example, Ref. [36]), or the related comments in Refs. [44–46], where a subtractive regularization approach is employed. This inconsistency between the Nijmegen

[9]The quoted scattering lengths have been computed for the fixed cutoff radius $r_c = 0.3$ fm for the N^{2}LO-Δ case and are accurate within the numerical error. The systematic uncertainty of taking a cutoff between 0.3 and 0.6 fm typically only influences the last digit (in the particular case of the $^1D_2$ scattering length we have a 0.005-fm^3 change in the previous cutoff window). Note that a factor of two in the cutoff corresponds to doubling the momentum space cutoff. Actually, using the "equivalence" $\Lambda = \pi/2r_c$ [41,55], we are testing the $\Lambda =$ 0.5–1-GeV region, which seems reasonable.

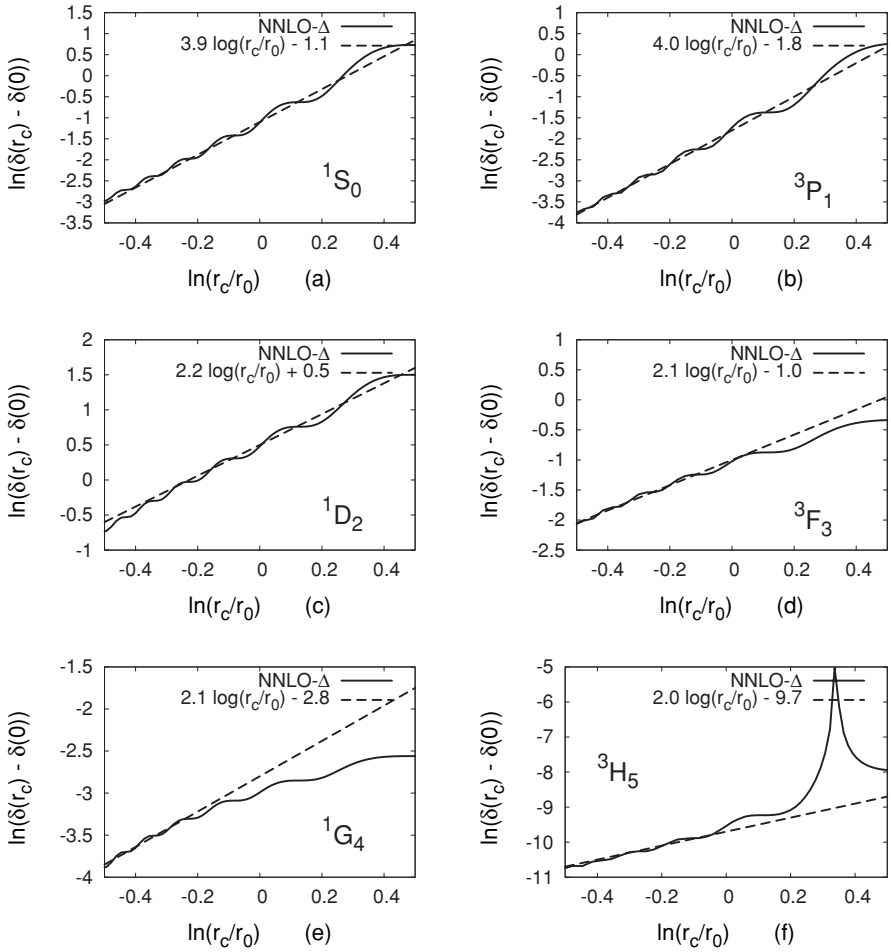

FIG. 5. (Color online) Dependence of the phase shifts with respect to the cutoff radius in the ${}^1S_0$-${}^1D_2$-${}^1G_4$ (left panel) and ${}^3P_1$-${}^3F_3$-${}^3H_5$ waves (right panel) at N^{2}LO-Δ for $E_{\rm LAB} = 200$ MeV. In the x axis we plot the natural logarithm of the ratio of the cutoff radius with respect to a scaling radius of $r_0 = 0.5$ fm, while the y axis displays the natural logarithm of the difference between the phase shift at the cutoff radius r_c and the phase shifts in the $r_c \to 0$ limit. The value of the phase shift in this limit is deduced by extrapolating from the scaling described in Eqs. (91) and (92). The figures also show a power law approximation to the cutoff dependence of the phase shifts, which confirm the expected scaling given by Eqs. (93) and (94). The approximation confirms the dominance of the chiral van der Waals component ($\sim 1/r^6$) of the interaction for cutoff radii below 0.8–0.9 fm ($\ln(r_c/r_0) \simeq 0.5$) for the lower partial waves ($l \leqslant 2$) and 0.5 fm ($\ln(r_c/r_0) \simeq 0.0$) for the higher partial waves ($l \geqslant 2$).

low-energy parameters and the chiral Δ potentials is explained by the fact that the Nijmegen phenomenological potentials do not contain either two-pion exchange contributions or Δ excitations, and was briefly commented in the previous references.

In Fig. 2, we show the results for the uncoupled triplet waves. We have taken as input parameter for the ${}^3P_1$ (${}^3D_2$) correlation the Nijmegen II scattering length [62], namely $a_{{}^3P_1} = 1.529$ fm^3 ($a_{{}^3D_2} = -7.405$ fm^5). Taking these values does not yield the better possible results for the ${}^3P_1$ (${}^3D_1$) wave, but generates renormalized results for the ${}^3F_3$-${}^3H_5$ (${}^3G_4$) waves. As it happened in the singlet case, the phase shifts for the higher partial waves are very similar to the values obtained in first-order perturbation theory either in the Δ-less [16] and Δ-full [17,53] cases.

In Figs. 3 and 4 we show the results for the coupled triplet waves. For the ${}^3S_1$-${}^3D_1$ correlation, we have taken as input parameters the deuteron binding energy $B_d = 2.224575$ MeV and D/S asymptotic ratio $\eta = 0.0256$, and the ${}^3S_1$ scattering length $a_{{}^3S_1} = 5.419$ fm. The scattering solutions are then constructed by orthogonality with respect to the deuteron wave function and the ${}^3S_1$ scattering state. The procedure is described in detail in Ref. [35], and was already used in Ref. [52] to construct the scattering solutions in the ${}^3S_1$-${}^3D_1$ channel for the Δ potentials of Ref. [53]. For $r_c = 0.3$ fm, we obtain the values $a_{E_1} = 1.953$ fm^3 and $a_{{}^3D_1} = 5.034$ fm^5 for the scattering lengths. The previous low-energy information yields much better results than the use of the Nijmegen scattering length for this channels ($a_{E_1} = 1.647$ fm^3 and $a_{{}^3D_1} = 6.505$ fm^5), which induce a spurious resonance at $k_{\rm cm} \simeq 100$ MeV when the N^{2}LO-Δ potentials are employed. This behavior can also happen when using the standard chiral potentials without explicit Δ degrees of freedom, as was discussed in Refs. [44–46]. The corresponding phase shift for the ${}^3D_3$ is slightly better than the one obtained in Ref. [53], whereas the ${}^3G_3$ phase and the ϵ_3 mixing parameter are quite similar to the ones obtained in the previous reference. The results for the ${}^3G_5$-${}^3I_5$ coupled channel are good in general with the exception of the ${}^3G_5$ phase in which only the threshold behavior is correctly reproduced.

In the case of the ${}^3P_2$-${}^3F_2$ waves, we renormalize these waves by fixing the scattering lengths to the values $a_{{}^3P_2} = -0.320$ fm^3, $a_{E_2} = 1.936$ fm^5, and $a_{{}^3F_2} = -1.289$ fm^7, which provide an acceptable description of the phase shifts for this channel (see Fig. 4). As happened in the ${}^3S_1$-${}^3D_1$ channel, the Nijmegen II values for the scattering lengths [62] do not yield good results with the NLO $-$ Δ and N^{2}LO $-$ Δ potentials. However, in the Δ-less theory the Nijmegen II scattering lengths generated good results at N^{2}LO [36], meaning that the discrepancy is from the long-range physics introduced by the Δ excitations. The ${}^3F_2$ phases show a strong relative cutoff dependence in the range $r_c = 0.6$–0.8 fm,

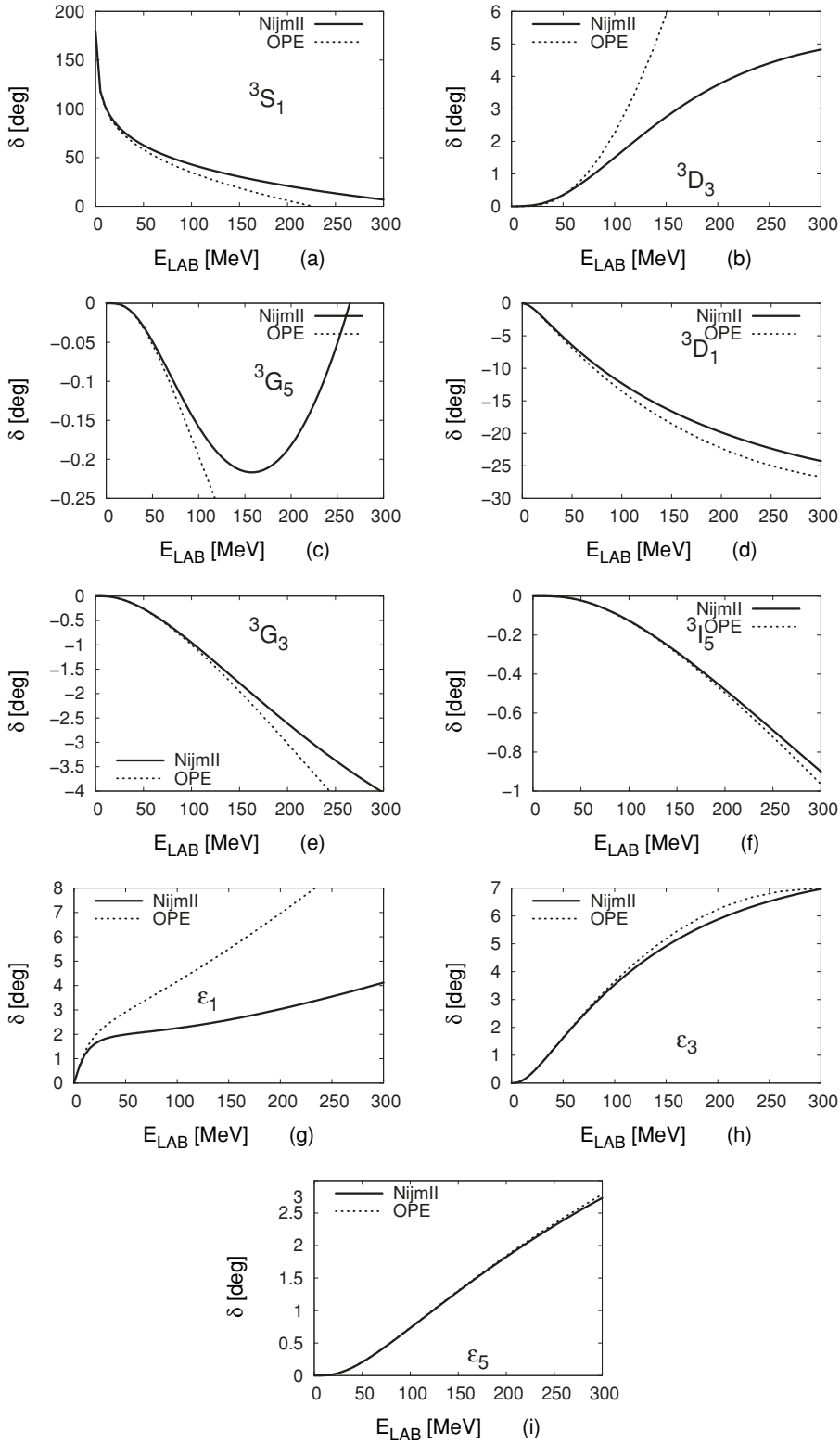

FIG. 6. $^3S_1$-$^3D_1$, $^3D_3$-$^3G_3$ and $^3G_5$-$^3I_5$ OPE coupled channel phase shifts. The $^3S_1$-$^3D_1$ wave is computed from orthogonality to the deuteron bound state and from the triplet scattering length $a_{^3S_1} = 5.419$ fm. The $^3D_3$-$^3G_3$ and $^3G_5$-$^3I_5$ coupled channels are computed from the partial-wave correlation given by Eqs. (49)–(52) *without* introducing new counterterms. The coordinate space cutoff is taken to be $r_c = 0.15$ fm.

although this is partly from the small value of this phase. As in the previous cases, the $^3F_4$-$^3H_4$ waves are very similar to those of Ref. [53].

Finally, in Fig. 5 we consider the cutoff dependence of the phase shifts in the form of a logarithmic (or Lepage's [30]) plot. For simplicity, we only consider two sets of correlated partial waves in detail, $^1S_0$-$^1D_2$-$^1G_4$ and $^3P_1$-$^3F_3$-$^3H_5$, a singlet and a triplet. For the other partial waves the cutoff dependence follows a similar pattern. According to Sec. IV E, for small enough cutoffs ($2m_\pi r_c \ll 1$) the convergence of the phase shift in the lower partial wave of the correlation (i.e., $^1S_0/^3P_1$ in this case) is given by

$$\log|\delta_A(k,r_c) - \delta_A(k,0)| \simeq 4\log r_c + C_A + f_A(r_c), \quad (93)$$

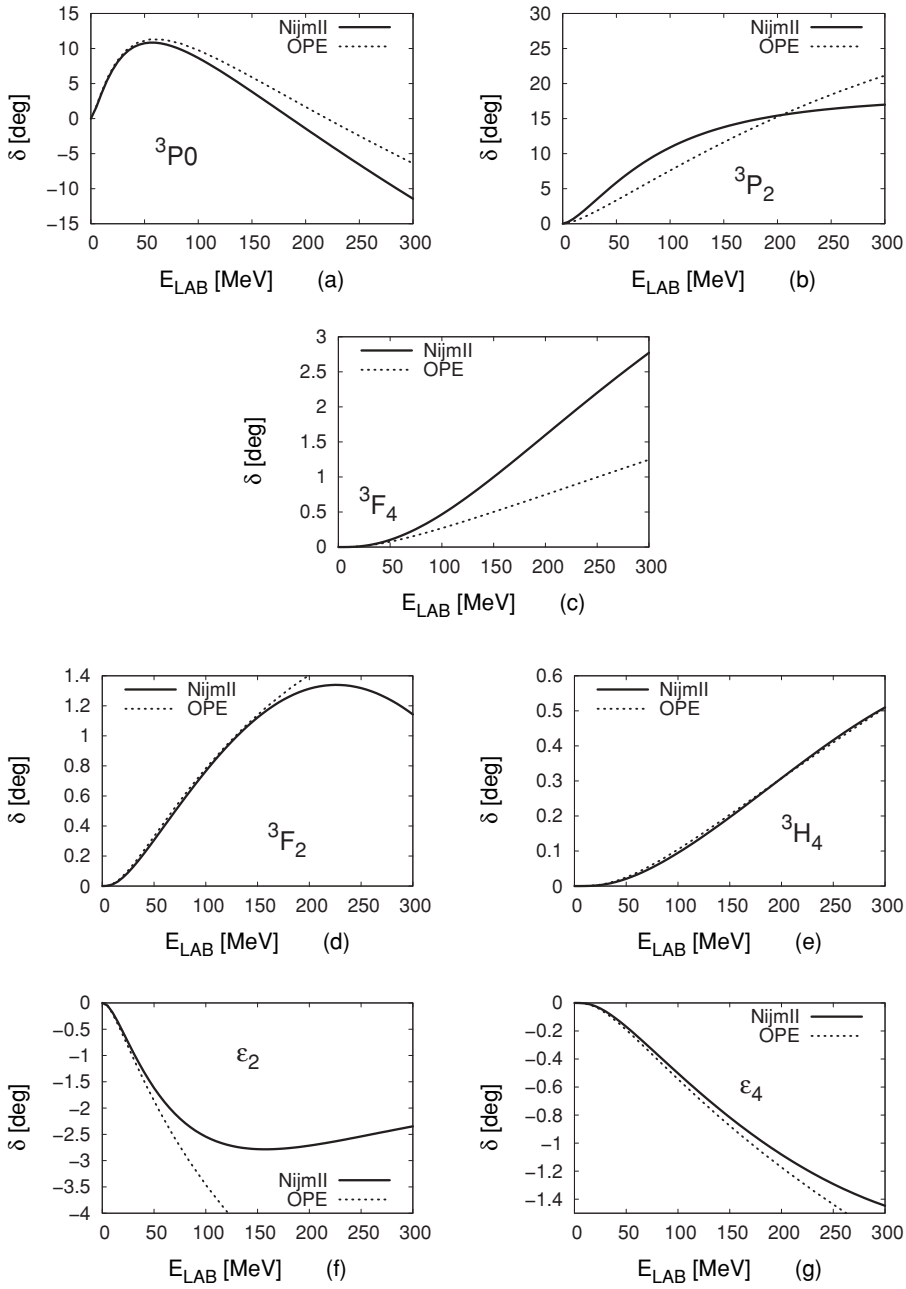

FIG. 7. $^3P_0$, $^3P_2$-$^3F_2$, and $^3F_4$-$^3H_4$ OPE phase shifts. The $^3P_0$ wave is constructed by fixing the scattering length to the value $a_{^3P_0} = -2.71$ fm^3, whereas the $^3P_2$-$^3F_2$ and $^3F_4$-$^3H_4$ waves are obtained from the partial-wave correlation described in Eqs. (49)–(52) *without* introducing any new counterterm. We take the coordinate space cutoff $r_c = 0.15$ fm.

where $A = {}^1S_0({}^3P_1)$, $\delta_A(k, r_c)$ is the phase shift computed at the cutoff radius r_c, $\delta_A(k, 0)$ the phase shift in the $r_c \to 0$ limit, C_A a constant, and $f_A(x)$ a small oscillatory contribution which takes into account the sine factor of the reduced wave function at short distances [see Eq. (18)]. As can be seen in Fig. 5, this behavior is indeed fulfilled up to $r_c \sim 0.8$–0.9 fm. In particular, the numerical factors multiplying the logarithms in the fits of Fig. 5 are very close to 4, indicating that the van der Waals contribution to the chiral potential dominates the behavior of the wave functions at short distances. For the higher partial waves in the correlation, the expected scaling is

$$\log|\delta_B(k, r_c) - \delta_B(k, 0)| \simeq 2\log r_c + C_B + f_B(r_c), \quad (94)$$

with $B = {}^1D_2/{}^1G_4({}^3F_3/{}^3H_5)$. In these waves the van der Waals dominance is apparent for cutoff radii below $r_c \simeq 0.5$–0.8 fm, with the lower bound corresponding to the most peripheral partial waves. It should be noted, however, that the appearance of van der Waals scaling in the renormalization group (RG) flow of the phase shifts for the higher partial waves does not imply that the phase shifts themselves are dominated by the $1/r^6$ piece of the interaction. The region in which the RG flow is driven by the chiral van der Waals force only amounts for a tiny contribution to the total phase shifts of the peripheral waves, as can be deduced from the large negative values of $\log|\delta(k, r_c) - \delta(k, 0)|$ in the case of the $^1G_4$ and $^3H_5$ waves (see Fig. 5). This feature fully agrees with the expectations of the renormalization approach.

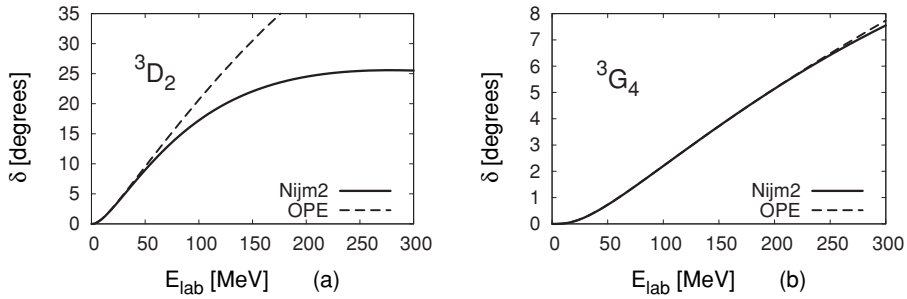

FIG. 8. $^3D_2$ and $^3G_4$ phase shifts computed from Eq. (71), using the $^3D_2$ scattering length as an input parameter and the OPE potential with a coordinate space cutoff $r_c = 0.15$ fm.

VI. CONCLUSIONS

In the present paper we have considered the relation between the renormalization of attractive singular potentials and the partial-wave expansion. Given that attractive singular interactions can be renormalized by including one counterterm per partial wave, each counterterm stabilizes the cutoff dependence in each one of the channels separately. Although this is a sufficient condition for renormalizability it is actually not necessary. We have shown that if the finite range (attractive singular) interaction is central, then it can be renormalized by means of a single delta-shell central potential in coordinate space, in contrast with the previous situation in which the predictive power is lost as there are an infinite number of partial waves. Of course, this result depends on the assumption that the unknown short-range potential which is represented by a single delta-shell counterterm is central. Phenomenological potentials do depend on the orbital angular momentum at short distances [4–7]. For this more general situation in which nothing can be assumed about the short-range interaction, the usual result of one counterterm per channel will be recovered.

Our analysis was carried out in coordinate space, which on the other hand was proven to be equivalent to momentum space calculations [41,55]. The particularly interesting issue of extending the correlated renormalization method to momentum space, not addressed in the present work, is left for future research. A possible clue might be provided by the observation that the high momentum behavior of the chiral potentials ought to reflect the partial-wave independence observed and exploited in the present paper at short distances, suggesting a common subtraction perhaps along the lines of Refs. [43–45].

We have extended the previous result to the case of a finite range potential containing a tensor piece, which is of great interest for the renormalization of nuclear forces in the effective field theory approach. In that case, the number of counterterms depends on the sign of the eigenvalues of the coupled channel potential. The application to the chiral *NN* potentials with Δ excitations is possible and straightforward, and only requires one to take into account the additional spin and isospin structure of the *NN* interaction. We stress that this is based on taking a counterterm structure based on the longer range OPE and TPE components of the interaction. For the order Q^2 and Q^3 Δ potentials of Ref. [53] a total of 11 counterterms is found to be needed to completely renormalize the interaction in all channels. This is only two more counterterms than what Weinberg's dimensional power counting dictates for the contact range interaction at the considered orders.

ACKNOWLEDGMENTS

We thank Alvaro Calle Cordón for discussions, Evgeny Epelbaum for a critical and careful reading of the manuscript, and Ulf-G. Meißner for correcting some references. M.P.V. is supported by the Helmholtz Association fund provided to the young investigator group "Few-Nucleon Systems in Chiral Effective Field Theory" (Grant No. VH-NG-222) and the virtual institute "Spin and strong QCD" (Grant No. VH-VI-231). The work of E.R.A. is supported in part by funds provided by the Spanish DGI and FEDER funds with Grant No. FIS2008-01143/FIS, and the Junta de Andalucía Grant No. FQM225-05. M.P.V. and E.R.A. are supported by the EU HadronPhysics2 Project.

APPENDIX A: PARTIAL-WAVE CORRELATIONS WITH THE ONE-PION EXCHANGE POTENTIAL

In this appendix we review the correlated renormalization for the one-pion exchange potential case, which corresponds to the leading order piece of the chiral potential. The OPE potential can be decomposed as

$$V_{\rm OPE}(\vec{r}) = \sigma\tau\, W_S(r) + S_{12}(\hat{r})\tau\, W_T(r), \tag{A1}$$

where the operators σ, τ and S_{12} were defined in Eq. (56) and $W_S(r)$ and $W_T(r)$ are given by

$$W_S(r) = \frac{m_\pi^2 g_A^2}{48\pi f_\pi^2}\frac{e^{-m_\pi r}}{r}, \tag{A2}$$

$$W_T(r) = \frac{m_\pi^2 g_A^2}{48\pi f_\pi^2}\left(1+\frac{3}{m_\pi r}+\frac{3}{(m_\pi r)^2}\right)\frac{e^{-m_\pi r}}{r}. \tag{A3}$$

As can be seen, the only singular component of the OPE potential is the tensor piece. Therefore partial-wave correlations only arise between attractive triplet partial waves. Specifically, there are three sets of correlated waves: (i) the $^3C_1$-$^3C_3$-$^3C_5$ case, which happens between coupled waves, (ii) the $^3P_0$-$^3C_2$-$^3C_3$ case, in which there is one uncoupled wave (the $^3P_0$) and the rest are coupled, and (iii) $^3D_2$-$^3G_4$ in which all waves are uncoupled triplets. All the coupled waves are of the attractive-repulsive type, and in total only three counterterms are needed to obtain finite scattering amplitudes for the OPE potential. Nonetheless, it should be noted that in usual EFT computations a fourth counterterm will be added to renormalize the $^1S_0$ wave. In any case, we will only consider those waves that can be related.

Contrary to the NLO-Δ and N^{2}LO-Δ cases, the cutoff radius must be quite small for the partial-wave correlations

to converge (especially between the $^3P_0$ and $^3P_2$-$^3F_2$ waves). In particular, we take $r_c = 0.15$ fm.

The $^3C_1$, $^3C_3$, and $^3C_5$ correlation is shown in Fig. 6. For this case, the $^3S_1$-$^3D_1$ wave function is renormalized by reproducing the triplet $^3S_1$ scattering length, $a_{^3S_1} = 5.419$ fm, a procedure that was described in detail in Ref. [39]. The other partial waves are generated by the renormalization conditions given in Eqs. (49)–(52). As can be seen, the description of the E_1 and $^3D_3$ wave is not especially good; these waves improve noticeably with the inclusion of two-pion exchange and the Δ. The remaining $j = 3$ and $j = 5$ phases do not differ too much from their NLO-Δ and N^{2}LO-Δ counterparts, as expected from the fact that peripheral waves are OPE dominated.

In Fig. 7 we show the resulting $^3P_0$, $^3P_2$-$^3F_2$ and $^3F_4$-$^3H_4$ phase shifts, which have been obtained by using the $^3P_0$ wave as the base wave, and where the $^3P_0$ scattering length was taken to be $a_{^3P_0} = -2.71$ fm^3. We can see that the $^3F_2$, E_2, and $^3F_4$ waves are not well reproduced with OPE alone and need the inclusion of the higher orders of the potential.

Finally, in Fig. 8 the $^3D_2$ and $^3G_4$ phase shifts are shown. The $^3D_2$ phase was renormalized to reproduce the Nijmegen II value of the scattering length, $a_{^3D_2} = -7.405$ fm^5. The OPE results for the $^3D_2$ are worse than those of NLO-Δ and N^{2}LO-Δ at moderate energies of the order of $E_{\rm LAB} > 150$ MeV. The $^3G_4$ phase is nicely reproduced with OPE alone.

[1] G. Brown and A. D. Jackson, *The Nucleon-Nucleon Interaction* (North-Holland Publishing, Amsterdam, 1976).
[2] R. Machleidt, K. Holinde, and C. Elster, Phys. Rept. **149**, 1 (1987).
[3] R. Machleidt, Adv. Nucl. Phys. **19**, 189 (1989).
[4] V. G. J. Stoks, R. A. M. Kompl, M. C. M. Rentmeester, and J. J. de Swart, Phys. Rev. C **48**, 792 (1993).
[5] V. G. J. Stoks, R. A. M. Klomp, C. P. F. Terheggen, and J. J. de Swart, Phys. Rev. C **49**, 2950 (1994).
[6] R. B. Wiringa, V. G. J. Stoks, and R. Schiavilla, Phys. Rev. C **51**, 38 (1995).
[7] R. Machleidt, Phys. Rev. C **63**, 024001 (2001).
[8] N. Ishii, S. Aoki, and T. Hatsuda, Phys. Rev. Lett. **99**, 022001 (2007).
[9] S. Aoki, T. Hatsuda, and N. Ishii, Prog. Theor. Phys. **123**, 89 (2010).
[10] S. Weinberg, Phys. Lett. B **251**, 288 (1990).
[11] P. F. Bedaque and U. van Kolck, Ann. Rev. Nucl. Part. Sci. **52**, 339 (2002).
[12] E. Epelbaum, H.-W. Hammer, and U.-G. Meißner, Rev. Mod. Phys. **81**, 1773 (2009).
[13] S. Weinberg, Nucl. Phys. B **363**, 3 (1991).
[14] C. Ordoñez, L. Ray, and U. van Kolck, Phys. Rev. Lett. **72**, 1982 (1994).
[15] C. Ordoñez, L. Ray, and U. van Kolck, Phys. Rev. C **53**, 2086 (1996).
[16] N. Kaiser, R. Brockmann, and W. Weise, Nucl. Phys. A **625**, 758 (1997).
[17] N. Kaiser, S. Gerstendorfer, and W. Weise, Nucl. Phys. A **637**, 395 (1998).
[18] E. Epelbaum, W. Glöckle, and U.-G. Meißner, Nucl. Phys. A **637**, 107 (1998).
[19] M. C. M. Rentmeester, R. G. E. Timmermans, J. L. Friar, and J. J. de Swart, Phys. Rev. Lett. **82**, 4992 (1999).
[20] J. L. Friar, Phys. Rev. C **60**, 034002 (1999).
[21] N. Kaiser, Phys. Rev. C **61**, 014003 (2000).
[22] N. Kaiser, Phys. Rev. C **62**, 024001 (2000).
[23] N. Kaiser, Phys. Rev. C **65**, 017001 (2002).
[24] N. Kaiser, Phys. Rev. C **64**, 057001 (2001).
[25] N. Kaiser, Phys. Rev. C **63**, 044010 (2001).
[26] D. R. Entem and R. Machleidt, Phys. Rev. C **66**, 014002 (2002).
[27] D. R. Entem and R. Machleidt, Phys. Rev. C **68**, 041001 (2003).
[28] E. Epelbaum, W. Glöckle, and U.-G. Meißner, Nucl. Phys. A **747**, 362 (2005).
[29] A. Nogga, R. G. E. Timmermans, and U. van Kolck, Phys. Rev. C **72**, 054006 (2005).
[30] G. P. Lepage (1997), arXiv:nucl-th/9706029.
[31] E. Epelbaum and U. G. Meißner (2006), arXiv:nucl-th/0609037.
[32] E. Epelbaum and J. Gegelia, Eur. Phys. J. A **41**, 341 (2009).
[33] S. Aoki, J. Balog, and P. Weisz, PoS**LAT2009**, 132 (2009).
[34] S. Aoki, J. Balog, and P. Weisz, J. High Energy Phys. **1005**, 008 (2010).
[35] M. Pavon Valderrama and E. Ruiz Arriola, Phys. Rev. C **74**, 054001 (2006).
[36] M. Pavon Valderrama and E. Ruiz Arriola, Phys. Rev. C **74**, 064004 (2006).
[37] M. C. Birse, Phys. Rev. C **74**, 014003 (2006).
[38] R. Machleidt and D. Entem, J. Phys. G **37**, 064041 (2010).
[39] M. Pavon Valderrama and E. Ruiz Arriola, Phys. Rev. C **72**, 054002 (2005).
[40] M. Pavon Valderrama and E. Ruiz Arriola, Ann. Phys. **323**, 1037 (2008).
[41] D. R. Entem, E. Ruiz Arriola, M. Pavon Valderrama, and R. Machleidt, Phys. Rev. C **77**, 044006 (2008).
[42] S. R. Beane *et al.*, Phys. Rev. A **64**, 042103 (2001).
[43] C.-J. Yang, C. Elster, and D. R. Phillips, Phys. Rev. C **77**, 014002 (2008).
[44] C. J. Yang, C. Elster, and D. R. Phillips, Phys. Rev. C **80**, 034002 (2009).
[45] C. J. Yang, C. Elster, and D. R. Phillips, Phys. Rev. C **80**, 044002 (2009).
[46] C.-J. Yang, C. Elster, and D. Phillips, PoS**CD09**, 064 (2009).
[47] D. B. Kaplan, M. J. Savage, and M. B. Wise, Phys. Lett. B **424**, 390 (1998).
[48] D. B. Kaplan, M. J. Savage, and M. B. Wise, Nucl. Phys. B **478**, 629 (1996).
[49] S. Fleming, T. Mehen, and I. W. Stewart, Nucl. Phys. A **677**, 313 (2000).
[50] S. R. Beane, D. B. Kaplan, and A. Vuorinen, Phys. Rev. C **80**, 011001 (2009).
[51] M. Pavon Valderrama, Phys. Rev. C **83**, 024003 (2011).
[52] M. Pavon Valderrama and E. Ruiz Arriola, Phys. Rev. C **79**, 044001 (2009).
[53] H. Krebs, E. Epelbaum, and U.-G. Meißner, Eur. Phys. J. A **32**, 127 (2007).
[54] E. Ruiz Arriola and A. Calle Cordon (2009), arXiv:0910.1333.

[55] M. Pavon Valderrama, A. Nogga, E. Ruiz Arriola, and D. R. Phillips, Eur. Phys. J. A **36**, 315 (2008).
[56] R. Machleidt, P. Liu, D. R. Entem, and E. Ruiz Arriola, Phys. Rev. C **81**, 024001 (2010).
[57] B. Long and U. van Kolck, Ann. Phys. **323**, 1304 (2008).
[58] M. Pavon Valderrama and E. Ruiz Arriola, Phys. Rev. C **74**, 054001 (2006).
[59] M. Pavon Valderrama and E. Ruiz Arriola, Phys. Rev. C **80**, 024001 (2009).
[60] E. Epelbaum, W. Glöckle, and U.-G. Meißner, Eur. Phys. J. A **19**, 125 (2004).
[61] E. Epelbaum, W. Glöckle, and U.-G. Meißner, Eur. Phys. J. A **19**, 401 (2004).
[62] M. Pavon Valderrama and E. Ruiz Arriola, Phys. Rev. C **72**, 044007 (2005).